PORTABLE IMPULSE MEASUREMENTS TO NON-DESTRUCTIVELY PREDICT THE INTEGRITY OF ADHESIVE JOINTS

T. S. SRIVATSAN
Materials Modification Inc.,
Falls Church, Virginia 22044

Final Report
(Period: 26 September 1986 to 26 March 1987)
Contract- N60921-86-C-0210
Department of the Navy
Naval Surface Weapons Center
Silver Spring, Maryland 20903

Naval Surface Weapons Center
Dahlgren, Va. • White Oak, Md.

UNCLASSIFIED
SECURITY CLASSIFICATION OF THIS PAGE

REPORT DOCUMENTATION PAGE

1a. REPORT SECURITY CLASSIFICATION	1b. RESTRICTIVE MARKINGS
2a. SECURITY CLASSIFICATION AUTHORITY	3. DISTRIBUTION/AVAILABILITY OF REPORT APPROVED FOR PUBLIC RELEASE DISTRIBUTION UNLIMITED
2b. DECLASSIFICATION/DOWNGRADING SCHEDULE UNCLASSIFIED	
4. PERFORMING ORGANIZATION REPORT NUMBER(S) MMI-SRI-0001-87	5. MONITORING ORGANIZATION REPORT NUMBER(S)
6a. NAME OF PERFORMING ORGANIZATION MATERIALS MODIFICATION INC. (6b. OFFICE SYMBOL (If applicable))	7a. NAME OF MONITORING ORGANIZATION NAVAL SURFACE WEAPONS CENTER
6c. ADDRESS (City, State, and ZIP Code) 2946 SLEEPY HOLLOW RD., SUITE 2H FALLS CHURCH, VA 22044	7b. ADDRESS (City, State, and ZIP Code) Head, Materials Evaluation Branch Code R-34, White Oak, MD 20903-5000 Attn : Dr Cliff Anderson
8a. NAME OF FUNDING/SPONSORING ORGANIZATION NSWC (8b. OFFICE SYMBOL (If applicable))	9. PROCUREMENT INSTRUMENT IDENTIFICATION NUMBER N 60921-86-C-0210
8c. ADDRESS (City, State, and ZIP Code) White Oak, MD 20903-5000	10. SOURCE OF FUNDING NUMBERS

PROGRAM ELEMENT NO.	PROJECT NO.	TASK NO.	WORK UNIT ACCESSION NO.
N00030	86	RC	65405

11. TITLE (Include Security Classification)
PORTABLE IMPULSE MEASUREMENTS TO NON DESTRUCTIVELY PREDICT THE INTEGRITY OF ADHESIVE JOINTS.

12. PERSONAL AUTHOR(S)
SRIVATSAN T.S.

13a. TYPE OF REPORT	13b. TIME COVERED	14. DATE OF REPORT (Year, Month, Day)	15. PAGE COUNT
FINAL	FROM 26 Sep to 26 Mar	26 March 1987	92

16. SUPPLEMENTARY NOTATION

17. COSATI CODES			18. SUBJECT TERMS (Continue on reverse if necessary and identify by block number)
FIELD	GROUP	SUB-GROUP	ADHESIVES, VIBRATIONS, DEBONDING, IMPULSE HAMMER

19. ABSTRACT (Continue on reverse if necessary and identify by block number)

The impulse-frequency response technique discussed in this report, successfully detected the presence of both macroscopic (debond) and microscopic (pores) flaws as reflected by a pronounced increase in damping (loss factor) with an increase in size, number and severity of the flaws tested. The presence of both macroscopic and microscopic flaws resulted in a degradation in the shear strength of the adhesive joint. The observed change in damping (loss factor) with cure time at the accelarated cure temperature was attributed to several competing mechanistic processes involving: a) shrinkage; b) chemical and physical characteristics of the adhesive; and c) thermal stresses. The pores and voids coupled with changes in the reaction kinetics of the adhesive mixture caused a large change in damping which was detected by the technique. Debond areas

20. DISTRIBUTION/AVAILABILITY OF ABSTRACT	21. ABSTRACT SECURITY CLASSIFICATION
☒ UNCLASSIFIED/UNLIMITED ☐ SAME AS RPT. ☐ DTIC USERS	

22a. NAME OF RESPONSIBLE INDIVIDUAL	22b. TELEPHONE (Include Area Code)	22c. OFFICE SYMBOL
Karen M. Jackson	202-394-2336	Code S 22

DD FORM 1473, 84 MAR 83 APR edition may be used until exhausted. All other editions are obsolete

SECURITY CLASSIFICATION OF THIS PAGE

☆ U.S. Government Printing Office: 1986—606-24.

19. ABSTRACT (Contd.)

within an adhesive joint were observed to cause a marked increase in damping with concomitant reduction in strength of the adhesive joint.

The damping was observed to increase exponentially with an increase in debond area. For different types, degree and intrinsic severity of flaws, a relationship was developed to predict strength of an adhesive joint from its dynamic properties. The actual fracture strength or load accords reasonably well with the predicted value obtained using this relationship.

PORTABLE IMPULSE MEASUREMENTS TO NON-DESTRUCTIVELY PREDICT THE INTEGRITY OF ADHESIVE JOINTS

T. S. SRIVATSAN

Materials Modification Inc.,

Falls Church, Virginia 22044

Final Report
(Period: 26 September 1986 to 26 March 1987)
Contract - N60921-86-C-0210
Department of the Navy
Naval Surface Weapons Center
Silver Spring, Maryland 20903

Naval Surface Weapons Center
Dahlgren, Va. • White Oak, Md.

TABLE OF CONTENTS

FOREWORD

This final technical report cover activities performed during the period October 01, 1986 to March 26, 1987 for the Naval Surface Weapons Center under U. S. Navy contract N60921-86-C-0210.

The contract is with Materials Modification Inc., (MMI), Falls Church, Virginia. Mr. Cliff Anderson is the U.S. Navy contract monitor. This report has been prepared by Dr. T. S. Srivatsan, MMI Principal Investigator and Project Manager for the program.

ACKNOWLEDGEMENTS

The author would like to acknowledge with thanks Mr. Raju Mantena, Department of Mechanical Engineering, University of Idaho, for his assistance and for the numerous stimulating discussions throughout all phases of this research. His untiring and ceaseless effort is responsible for the timely completion of this project.

I would also like to express my thanks and appreciation to Professor Ronald F. Gibson and Professor T Alan Place, University of Idaho, for their interest and time expended in this project, and for the many useful suggestions. Their academic insight has helped improve the overall quality of work executed.

It is a pleasure to thank Dr. T. S. Sudarshan for his role in lighting up the road for this work, his guidance and constructive criticisms.

Finally, I would like to extend special thanks and express gratitude to Colonel (R) Donald A. Tapscott, President, Materials Modification Inc, for his sustained encouragement since the time of initiation of this project. Without his understanding and support completion of this work would not have been possible.

LIST OF TABLES

LIST OF FIGURES

ABSTRACT

This investigation was undertaken to evaluate the feasibility of using an impulse-frequency response technique for the non-destructive evaluation of the structural integrity of adhesively bonded joints.

Defects of several types are frequenctly encountered in adhesive joints resulting in degradation. Some of the most common defects are: complete voids or disbonds, porosity, improper curing of the adhesive, and poor adhesion between the adhesive layer and the adherend. In the presence of these defects, effective determination of adhesive bonded joint durability is essential for reliable component design and realization of advanced performance.

In this Phase I study, the contributions from intrinsic defects caused by improper curing, induced porosity and improper surface preparation on the performance of double-lap adhesive joints bonded with a structural epoxy adhesive is examined. The double-lap adhesively joined specimens were excited in flexural vibration by an electromagnetic hammer with a force transducer at its tip. The specimen response was measured with a non-contacting eddy current probe. A Fast Fourier Transform analyzer was used for data acquisition and computation of the loss factor (a measure of damping). Strength of the adhesive joint was determined for the different types and levels (size and volume) of defects. The damping was found to correlate well with strength, with

strength decreasing and damping increasing with size, number, volume and severity of defects. The micromechanisms governing the performance and durability of bonded joints is discussed in terms of the specific role of curing time, curing temperature, adhesive degassing time, surface preparation, reaction kinetics, adhesive chemistry, adhesive thickness, and level and type of load. The potential for using the impulse technique for non-destructive evaluation of the structural integrity of adhesive joints is highlighted.

1. INTRODUCTION

Adhesive bonding of metals has in recent years engendered considerable interest in the aerospace and transportation industries, and has great potential for application to other areas of manufacturing. There are many reasons for the application of adhesive bonding: separation of dissimilar materials to prevent galvanic corrosion, absorption of vibration from one component to another [1], and joining cold rolled or heat sensitive materials. Besides providing weight savings, reduced part count and manufacturing cost effectiveness [2], adhesive bonding is attractive because it can offer considerable advantages over other forms of joints. For instance, the transfer of stress occurs over the entire bond area, thereby, avoiding the stress concentrations that occur with welding, riveting and fastening with screws [3].

Use of adhesive bonding simplifies construction and obviates the harmful effects of elevated temperatures associated with welding and brazing, resulting in improved appearance and reduced weight. In spite of its potential advantages, progress in the use of adhesive bonding in primary structures [4] has been painfully slow and hampered by:

(i) an inability to guarantee that the completed joint is of adequate strength, and

(ii) lack of adequate non-destructive testing procedures

without which the reliability of a structure cannot be guaranteed.

The durability or permanence of a bonded joint in service is an important consideration in the acceptance of an adhesive joint for a particular end use. Ideally, the most reliable information on the durability characteristics of a given adhesive or adherend-adhesive system need to be developed by subjecting the test sample to conditions comparable to those of the glued product in service. However, such long term tests are impractical. Consequently, greater reliance must be placed on results obtained from short-term accelerated tests. Non-destructive test techniques could predict the strength of the bond. This is very difficult to achieve, partly because a direct measurement of strength cannot be non-destructive. Hence, it is advantageous to correlate strength with other properties such as stiffness, damping and bond area. Previous research on composite materials by Mantena and co-workers [5] has shown that damping is quite sensitive to matrix cracking. The impulse-frequency response technique was found to be quite effective for such studies [8,9]. Further, the stress distribution in a typical adhesive joint is far from uniform, so the strength is much more sensitive to the integrity of some areas of the joint than to the others [6]. The basic premise of the work reported here was that measurements of the dynamic mechanical properties of an

adhesively bonded member could be used to indicate the structural integrity of the joint.

A plausible approach to bridging the gap between accelerated non-destructive test data and real-time results is a fundamental understanding of the intrinsic properties of the elements constituting an adhesive joint, and their contribution both separately and jointly to the overall integrity of the bonded assembly. The actual defect types which occur in bonded structures are [7]:

(a) Complete voids, disbonds or porosity.

(b) Poor adhesion, i.e., a weak bond between the adhesive and one or both the adherends.

(c) Poor cohesive strength, i.e., a weak adhesive layer.

Voids or large gas bubbles in the adhesive are caused either by a lack of adhesive or by the presence of foreign matter on the adherends, or even in, the adhesives. Porosity of the adhesive is similar to voiding except that the size of the bubbles are much smaller. It is usually caused by volatiles or gases trapped in the adhesive. Porosity is a major problem in composite adherends and occurs when the absorbed moisture vaporizes during the cure cycle to produce bubbles in the adhesive.

Disbonds or zero-volume bonds (area where no bond exists but also no adhesion is present), can occur due to:

(i) The presence of a contaminant, such as grease, on an adherend,

(ii) a poorly prepared adherend surface, and

(iii) environmental degradation after manufacture.

Degradation due to the environment takes place at an interface between the adhesive and the adherends, causing the bonds to fail. The surfaces of a disbond are generally in close proximity, or are touching, but are incapable of transferring load from the adherend to the adhesive.

Improper curing, that is, too low a curing temperature, or inadequate time at the required curing temperature or improper mixing of the adhesive components are factors responsible for variation in physical properties of a particular adhesive due to insufficient cross-linking of the polymer. Consequently, if cohesive properties are required, destructive tests are often performed on specimens manufactured under the same conditions as the actual structure, while non-destructive tests are preferred for the evaluation of an adhesive-adherend interface. Failure of adhesively bonded joints is often due to catastrophic crack propagation originating from inherent flaws, such as adhesive cracks, voids, porosity and disbonds, or impurities on the adhesive-adherend interface.Complete characterization of an adhesive joint requires a critical examination of the influence of these flaws on joint performance and durability.

In this Phase I research effort, flaws or defects of different type, degree and severity were created in an adhesive joint through careful control of processing

variables. Composite specimens comprised of two steel adherends held together by a double-lap adhesive joint, were non-destructively evaluated using an impulse-frequency response technique [8,9]. The dynamic properties (damping and resonant frequency) of the bonded specimen were correlated with the static shear strength of the adhesive joint. Changes in these properties with the number, size, volume and intrinsic severity of the flaws are discussed in terms of the specific role of several factors involving curing time, curing temperature, adhesive degassing time, surface preparation and contact area of the adhesive with the adherend. Potential use of the impulse technique for the non-destructive evaluation of the structural integrity of adhesive joints is rationalized.

2. SPECIMEN DESIGN AND CONFIGURATION

In order to accomplish the objective of dynamic analysis of adhesive joints, a specimen which is: (i) simple in design, (ii) easy to fabricate, and (iii) easy to operate with is essential. A double-lap specimen configuration with provisions for clevis pins (Figure 1) facilitates loading of the test specimen in a MTS servohydraulic structural test machine. The material chosen for the adherend was a hot rolled structural steel having a fine grain size, while the adhesive was a mixture of Epon 815 epoxy and Hardener V-40.

In several independent studies, Gibson and co-workers

[10,11] have found the damping of Epon 815 epoxy to be frequency dependent in the range 0-250 Hz as indicated in Figure 2. Above 250 Hz, the loss factor (a measure of damping) is essentially independent of frequency. Since degradation of the adhesive joint will cause a change in the resonant frequency, the specimen design should be such that any changes in damping would be entirely due to the degradation and not due to changes in frequency. Thus, a specimen is required which would resonate at frequencies above 250 Hz. Accordingly, the overall length of the composite specimen (two steel adherends held together by an adhesive joint), the thickness of the adherend, the thickness of the adhesive and the length of the adhesive were chosen after careful calculation, in order to obtain resonant frequencies of over 250 Hz. The specimen design chosen eliminates the need for the adhesive along the 'bottom wall' of the receiving ('female') adherend of the composite specimen in order to minimize transverse tension effect during loading of the specimen. The specimen configuration is such that the adhesive is only along the clevis walls of the adherend and is subject to pure shear loading. Dimensions of the composite specimen are summarized in Appendix A (Figure 1).

The specimen configuration and design chosen minimizes frequency effect due to the epoxy, and the impulse measurements would give good resonant peaks that would

enable the integrity of the adhesive joint to be established using the flexural vibration technique.

3. ADHESIVE SELECTION AND PROPERTIES

A major function of an adhesive is to fasten parts together. This is done by transmitting stresses from one member of a joint to another in a manner that distributes the stresses much more uniformly than can be achieved with conventional, mechanical fasteners. Consequently, adhesives permit the fabrication of structures that are mechanically equivalent to, or stronger than, conventional assemblies. Structural or performance adhesives are primarily load-bearing adhesives. That is, they add strength to the products being bonded. The ultimate choice of an adhesive for a given application depends on:

(a) the material to be joined,

(b) intended use of the bonded material, and

(c) conditions under which it is to be assembled.

Epoxy is a type of structural adhesive that is most commonly used.

The Epon 815 epoxy resin/V-40 hardener system chosen for this study was obtained from Shell Company, Atlanta, Georgia. To characterize the elastic modulus of the epoxy, three point bend tests were carried out under total stroke control on a MTS servohydraulic test machine. Figure 3

shows a typical load-displacement curve, and the modulus of elasticity obtained was 0.244×10^6 psi.

Specimens of the Epon material were also deformed in uniaxial tension under total stroke control in the MTS machine, and the resultant load-displacement curve is exemplified in Figure 4. The elastic modulus obtained from the extensometer trace was 0.304×10^6 psi. The modulus of elasticity values determined from the bending and tension tests compare favorably with the storage (dynamic:flexure) modulus obtained from Figure 5. The stiffness properties of Epon 815 epoxy are summarized in Table 1.

4. JIG DESIGN AND ASSEMBLY

It was necessary to design a jig which would:

(a) enable proper alignment of the test specimen,

(b) facilitate pouring of the adhesive,

(c) control the adhesive thickness and thus enable a symmetric joint of uniform thickness to be obtained, and

(d) hold the specimen with adhesive in a precise upright position during the process of curing.

In order to facilitate rapid production of adhesively joined steel specimens under controlled conditions, the jig was designed to accomodate five test specimens in each setting (Figure 6). To provide ease in handling and to ensure separation of the jig after the adhesive has cured,

the jig consists of a die split into two halves (Figure 7). The two halves are mounted on a base plate. Schematics of the die and the base plate are shown in Figures 8 and 9. The entire assembly of the jig comprising of the split-dies, the base plate and the shims is shown in Figure 10. To ease separation of the split-dies after the adhesive has cured, a film of silicone mold release was smeared on the face (portion) of the test specimen adjacent to the die. Great care was taken to ensure that the mold release did not come in contact with the surfaces being bonded, or indeed with the adhesive.

Provisions for the insertion of steel shims were also made in the jig. The shims: (i) minimize leakage of the adhesive, (ii) control the amount of adhesive shrinkage, (iii) aid in obtaining a symmetric double-lap joint through careful control of adhesive thickness, and (iv) prevent the 'male' adherend of the composite specimen from tilting during the process of curing.

5. SURFACE PREPARATION

Solid surfaces have a texture which is characterized by waviness, roughness and indentations such as cracks and pits. Such effects can influence adhesive spreading and bond strength. Surface indentations may interfere with wetting if they retain trapped air or selectively concentrate solvents from the adhesive. Besides being

highly textured, solid surfaces in the normal state are often impure. Most often, the surface of a metal is covered with a layer which has quite different properties from the bulk [12]. This layer may contain grease, processing lubricants, oxidation products or incidental contaminants. Hence, the strength of an adhesive joint is limited by forces between this layer and the adhesive, or between this layer and the metal or by the cohesive strength of the layer; whichever is the weakest.

The surface layer in its original state has a deleterious effect on adhesive bond strength and needs to be removed by suitable treatment before bonding [13]. For example, if unprepared steel is bonded, it is not the iron-carbon alloy that is bonded, but the iron-oxide layer on the surface. The iron-oxide (rust) layer separates readily from the base metal, and is therefore detrimental to strength of an adhesive joint. Regardless of how strongly the adhesive bonds to the rust on the surface, it will do no good if the rust separates from the metal.

In order to render the steel adherends receptive to bonding, the ASTM Standard Practice for preparation of metal surfaces for adhesive bonding, D2651-798 was used. The suggested ten minute etch with strong sulfuric acid-sodium dichromate solution was replaced by polishing the surfaces with 400 grit silicon carbide paper wetted with dilute sulfuric acid. The residue was washed with warm water and

the adherends stored in acetone until use. This procedure enhances the bond strength by:

(i) removing rust and exposing a bare steel surface, and

(ii) roughening the surface, thereby, increasing the area for bonding.

Since adhesive bonding depends on electrostatic forces between the adhesive molecules and the metal atoms, an increased surface area means an increase in the number of sites available for bonding, which in turn results in a stronger joint.

Good wetting of the adherend surface is essential for the development of reliable bonds. Wetting refers to the intimate association of a liquid (the adhesive) with a solid (the substrate). This intimacy of contact implies a sort of 'electron cloud mixing' between the materials [14]. A clean metal surface allows the water molecules to shift some of their attractive forces for each other to attraction for the substrate. Without this wetting, strong bonds are impossible. A clean metal surface has an extremely high critical surface tension, of the order of several hundreds dynes per centimeter. As a consequence, adhesives of low surface tension have little trouble wetting the adherend surfaces. Prior to bonding the adherend surfaces were checked for cleanliness by the water-break-free method (Figure 11).

6. ADHESIVE PREPARATION AND CURING

The adhesive was prepared in accordance with manufacturers instructions and due regard was given to handling precautions for the epoxy resin material used. Epon 815, a plasticised liquid epoxy resin was mixed with Hardener V-40, in the proportion of 100 parts of Epon and 80 parts of Hardener by weight. All weight measurements were made using a Mettler Instrument Corporation, Type P163, electronic analytical balance with a precision of 0.001 grams (Figure 12). The adhesive was prepared at ambient-room temperature, i.e., 23 C (75 F) in laboratory air environment (relative humidity, 65 percent), using weight proportioning. The resin and hardener were thoroughly mixed for 20 seconds to ensure a uniform mixture. Following mixing, the adhesive was degassed under vacuum (Figure 13) at a temperature of 100 C (212 F) for a period of seven minutes. The viscous adhesive was then poured into the 'female' adherend positioned in the jig (Figure 14). The 'male' adherend was lowered (Figure 15) into the double-lap female adherend to form the required joint. The assembled jig with adherends in position was placed in a furnace for curing at an elevated temperature of 100 C (212 F) (Figure 16). The elevated temperature facilitates acceleration of the cure process. The Epon 815 epoxy does cure at ambient-room temperature. The cure time is the amount of time the specimen is in the oven. Cure schedules with cure time

settings of 60 minutes, 120 minutes, 180 minutes and 240 minutes (complete cure) at the cure temperature (100 C) were used. For each individual cure condition a fast cool-down rate was chosen, which is stimulated by turning the oven off, leaving the door open and allowing the jig and specimen assembly to reach ambient-room temperature. The cured composite specimens were then stored for 48 hours in a low humidity environment in order to minimize any environmental effect on bond stability (Figure 17). This was accomplished by storing the specimens in a desiccator.

7. DYNAMIC TESTING: IMPULSE TECHNIQUE

In the Fast Fourier Transform (FFT) based impulse technique [8,9], the transfer function or frequency response function for the specimen is obtained by tapping the specimen with an electromagnetic impulse hammer which has a piezoelectric force transducer attached to its tip (head) (Figure 18). The specimen response is sensed by a non-contacting eddy current proximity transducer positioned at a desired location away from the nodal points. Measurement of response near the nodal points for the nodes to be tested is avoided since such measurements would consist primarily of noise. The input signal from the force transducer and the response signal from the motion transducer are fed into the FFT analyzer, and the desired frequency response function on

the desired frequency span is displayed on the screen in real time.

The loss factor (a measure of damping) for each resonant frequency is obtained by using the half-power bandwidth technique (Figure 19):

$$\eta = (\Delta f)/f_n \quad \ldots\ldots\ldots (1)$$

where

Δf = bandwidth at the half-power points of resonant peak of the nth mode.

f_n = resonant frequency of the nth mode.

The half-power points are found at 3dB below the peak value of the transfer function for a specific mode when a logarithmic scale is used, or at 0.707 of this peak value when a linear scale is used. The data reduction is carried out by using a Hewlett Packard (HP-85) computer which is connected to the FFT analyzer (HP3582A). After the desired number of ensemble averages (which removes extraneous noises, and to some degree non-linearities and distortion effects), the desired transfer function is displayed on the screen of the FFT analyzer (Figure 20). Use of the zoom feature on the FFT analyzer makes it possible to analyze the peaks more accurately (Figure 21). A computer program written in BASIC for the HP 85 computer was used for data acquisition and reduction (Figure 22). The program reads the binary values from the memory of the FFT analyzer, makes the corresponding transformations to the current scale, finds the points on either side of the half-power points,

and locates the half-power points by interpolation. The resonant frequency, f_n, and the half-power bandwidth are then used in Equation (1) to find the loss factor.

In the flexural vibration test, the adhesive end of the composite specimen was clamped to a depth of an inch (1.0"), while the adhesive and the other end of the composite specimen were free, giving a fixed-free end condition (Figure 23). A non-contacting eddy current probe was positioned at the free end. In order to obtain reproducible impulses, an electromagnetic hammer with a piezoelectric load cell (PCB 208A03) was used to impact the specimen at the free end.

The advantages of using an electromagnetic hammer having as piezoelectric force transducer attached to its tip are [8]:

(i) minimization of the variability of the excitation in successive measurements due to difference in the input force and the striking angle, giving a more reproducible impulse while the non-linearities and extraneous noises are minimized (the coherence function being improved). The electromagnetic hammer facilitates reduction of the input force so that the resulting specimen amplitude is low enough to eliminate significant air damping. The force signal is however, adequate to trigger the FFT analyzer.

(ii) The input is repeatable so that the response

spectrum is nearly the same for the repeated tests. In the vicinity of the resonant peaks, the shape of the transfer function spectrum after ensemble averaging tends to approach that of the single test response spectrum. Besides, the loss factors obtained using the bandwidth technique on the response spectrum do not vary with respect to those values obtained using the transfer function spectrum after ensemble averaging.

8. EFFECT OF CURING ON PERFORMANCE OF ADHESIVE JOINT

For the adhesive chosen in this study (Epon 815 epoxy), curing depends more on chemical reaction rather than on mere loss of solvent or crystallization. Consequently, curing is greatly hastened or accelerated by an increase in temperature over a period of time.

Composite specimens with the adhesive cured over a range spanning the under-cured (low stiffness and strength) to fully cured condition (high stiffness and strength) were obtained by varying the curing time. Dynamic tests in the flexural mode were conducted on the composite specimens using an impulse-frequency response technique. The tests were performed at ambient, room temperature (23C). Prolonged delay in testing following accelerated curing for different time periods was avoided since it could result in self-correction of poor cure, i.e., the chemical reaction

could continue at the ambient temperature, albeit slowly. On the other hand, tests showed that properties changed significantly within the first few hours after curing, as the material reached equilibrium. Thus, in order to minimize contributions from prolonged delay or non-equilibrium conditions, the dynamic tests were conducted following a 48 hour delay period for the different cured conditions.

The effect of cure time (at constant cure temperature of 100 C) on dynamic properties is summarized in Table 3. From this Table, it is observed that undercuring, i.e., curing for time periods less than the prescribed time period (240 minutes) results in an increase in damping (loss factor). The increase is as high as 35 pct. for the specimens cured for only 60 minutes. At cure time of 120 minutes the increase in damping was only marginal. The marginal increase in damping suggests that the adhesive achieves a stable and favorable molecular network structure at time periods beyond 120 minutes. As a result, there occurs a complete bonding of the adhesive to the steel adherend. The variation of loss factor with cure-time is exemplified in Figure 24.

Several mechanistic explanations can be put forth to account for the transient change in damping. The high temperature, short-time cure schedule represents a highly unsteady condition favoring the build-up of large thermal stresses. However, these stresses are most likely relieved

during the slow cool-down rate and is an appealing rationale for the adhesive developing a more stable and favorable molecular structure [15].

Variation in the degree of shrinkage of the adhesive is a plausible reason for the observed change in damping and stiffness. An intensive study by Hylands and Sidwell [16] on the effect of glue-line thickness on bonded steel-to steel joints revealed that the shrinkage of the adhesive is a function of its thickness. For joint thickness greater than 0.06 inch the adhesive shrinkage was observed not to degrade strength. Since the thickness of the adhesive in the adhesively joined composite steel specimen used in this study is 0.04 inch, contributions to damping from shrinkage if any, cannot be ruled out.

The other reason for the observed trend in damping (loss factor) could be due to a combination of the chemical nature and the physical characteristics of the adhesive in relation to the adherend. Controlled wetting and penetration are two important prerequsites which need be satisfied for the formation of a joint of sound integrity. For these conditions to be fulfilled, an appropriate viscosity level is imperative [17]. Attainment of this viscosity level is contingent upon:

(1) components of the adhesive,

(2) cure temperature, and

(3) cure time.

The first two factors were held as constant as possible in this experiment. Thus, the over-riding or controlling factor is the cure time and it was observed to have only a marginal influence on joint performance.

Results of the dynamic tests reveal only a marginal change in resonant frequency with cure-time (Table 3). While the different degrees of cure do not cause any dramatic change in the 1st mode resonant frequency (Figure 25), the corresponding change in loss factor is significant for the 60 minute cure (Figure 24).

The shear strength of the adhesive joint was determined by uniaxial loading of the composite specimen in a servohydraulic testing machine. Failure was taken to be the point at which the 'male' adherend separates from the 'female' adherend due to failure of the adhesive layer. Provision was made at the adhesive end of the composite specimen to accomodate a clip-gage type extensometer (Figure 26) which measures the relative movement of the adhesive layer during deformation of the composite specimen under a uniaxial (tensile) load. A load-displacement curve was obtained on an X-Y recorder. From the load-displacement curve, the shear stress (τ) and shear strain (γ) at failure were determined.

The adhesive cured for 60 minutes at the temperature of 100^{o}C will henceforth be referred to as an under-cured condition. It is observed that the shear strength is lowest for the under-cured condition. When compared with the

strength of the completely cured adhesive joint, a degradation in shear strength is observed for the under-cured adhesive (Figure 27). The severity of the under-cured condition is responsible for the degradation in strength which is as high as 55 percent (Table 3). A decrease in strength of the adhesive joint results in a concomitant increase in damping of 35 pct (Table 3). For the specimens cured for 120 minutes and 180 minutes, the adhesive joints are observed to be stronger than the perfectly cured specimen. This trend confirms the earlier observation that the adhesive achieves a stable molecular structure at times beyond 120 minutes. A comparison of the shear stress-shear strain curves for the different cure times is made in Appendix II (Figure 1).

In retrospect, it appears that the EPON 815 epoxy was not a very good choice for the curing time studies. Since this epoxy cures at ambient, room temperature, the elevated temperature cure only serves to accelerate the cure process. An elevated temperature cure epoxy would have shown more significant changes in properties for different curing times.

9. EFFECT OF POROSITY ON JOINT PERFORMANCE

Porosity is caused by volatiles and entrapped air in the adhesive (Figure 28). The degree of porosity in the adhesive was controlled by varying the degassing time of the

liquid adhesive. By degassing the adhesive under vacuum for times less than the time prescribed for complete degassing, air and product gas resulting from the reaction between the epoxy and hardener are trapped in the adhesive mixture. Thus, the volume of air and reaction gas pockets (pores) are likely to be greater when the adhesive mix was not degassed.

Preliminary tests revealed an migration of the pores to the top portion of the double-lap joint and eventual breakdown of these pores and voids during curing at an elevated temperature (100 C). Therefore, to minimize the depletion of induced pores and voids by the elevated temperature cure, the porosity specimens were allowed to cure at ambient temperature (26 C) for a period of 7 days.

When compared with a totally degassed mixture (7 minutes), the adhesive mixture which was not degassed (referred to as 0 minutes in Table 4 and Figures 29-31) prior to pouring caused a drastic change in dynamic properties of the joint. The loss factor for the different adhesive degassing times (0, 2 and 7 minutes), reveals an increase as high as 445 percent for the composite specimen whose adhesive was not degassed (0 minutes) (Figure 29). The change in first mode resonant frequency caused by the presence of pores and voids was only marginal as shown in Table 4 and exemplified in Figure 30.

The impulse-frequency response technique successfully detects and magnifies the presence of pores and/or voids as

is evident by the large change in damping (loss factor). The volume fraction of flaws caused by the entrapped air and product/reaction gases, i.e., pores and voids, results in a marked degradation in shear strength of the adhesive joint as summarized in Table 4. The volume fraction of pores and/or voids in the undegassed adhesive mixture coupled with contributions from adhesive chemistry and changes in reaction kinetics, results in the adhesive joint having inferior strength (Figure 31) and exhibiting increased damping. While the degradation in strength is 75 percent, the concomitant change in damping is as high as 445 percent. It seems likely that the pores at an adhesive-adherend interface, act as debond area and consequently, degrade the strength of an adhesive joint. From Figure 29 and 31, and Table 4, it is evident that degassing the adhesive mixture for even short periods of time, say 2 minutes, is adequate to reduce the total amount of entrapped air in the adhesive mixture, and complete the reaction kinetics of the adhesive mixture thus, minimizing contribution from these factors and resulting in only a marginal change in damping and frequency. The detection of pores and contribution from changes in reaction kinetics of the adhesive are further discussed in Section 12. A comparison of the shear stress-shear strain curves for the different degassing times is made in Appendix II, Figure 2.

10. EFFECT OF SURFACE PREPARATION (Area of Debond) ON JOINT PERFORMANCE

Surface debonds are an alternative form of voids, often caused when the adhesive fills or wets the adherend unevenly. Such a defect (Figure 32) is a direct result of poor surface preparation. Areas of total debond were created by applying mold release agent to the adherend prior to pouring the adhesive. The composite specimens were cured for 60 minutes at an elevated temperature of 100 C.

The total area of debond was varied, with composite specimens having no debond, to composite specimens having 25 %, 50 %, and 75 % of the adherend contact area debonded on both sides of the double-lap joint. It is observed that when even a small fraction (25 percent) of the total adherend contact area is debonded there occurs a significant change in the loss factor (Table 5 and Figure 33), and resonant frequency (Table 5 and Figure 34).

An increase in the percentage of total debond area results in an appreciable increase in damping. The increase in loss factor for specimens with 75 percent of the adhesive-adherend contact area debonded is of the order of 1894 percent! Coulomb friction or impact due to opening and closing of the debond interface during vibration is believed to be the cause of the additional damping. A corresponding degradation in shear strength of the adhesive joint with an increase in debond area is shown in Table 5 and depicted in

Figure 35. The impulse-frequency response technique used to non-destructively evaluate the dynamic properties of the composite specimens reveals an exponential increase in damping (loss factor) with an increase in debond area (Figure 33). The degradation in strength of the adhesive joint with increase in debond area correlates well with the increase in damping. A comparison of shear stress-shear strain curves for the different levels of debond is made in Figure 3 of Appendix II.

The variation of dynamic properties (loss factor and resonant frequency) with joint shear strength for composite specimens having different types and levels of built-in or induced defects caused by (i) improper curing, (ii) varying time of adhesive degassing, and (iii) improper surface preparation, is succintly summarized in Figures 36 and 37. The impulse-frequency response technique reveals a dramatic increase in damping (loss factor) with increasing size, number, volume and severity of defects. There also occurs a degradation in strength of the joint with increasing severity of the flaws or defects. For the composite specimens investigated in this study, the variation of loss factor (η) with joint shear strength (τ) can be expressed by the relationship:

$$\eta = 20.349\ (T)^{-0.877} \quad \ldots\ldots\ (2)$$

The change in resonant frequency with increasing size, number, volume and severity of the flaws is only marginal (Figure 37). With increasing severity of the flaws, the

joint strength is low and the corresponding resonant frequency is lower for specimens having smaller fraction of defects or flaws. The variation of resonant frequency (F) with joint shear strength (T) is best expressed through the relationship:

$$F = 18.261\ (T)^{0.348} \quad \ldots\ldots\ (3)$$

11. EFFECT OF STATIC PRE-LOAD ON JOINT DURABILITY

In an attempt to evaluate the effect of loading on the durability of an adhesively bonded member, composite specimens were subjected to loads (referred to henceforth as pre-loads) of different fraction or percentage of the estimated failure load. The dynamic properties (resonant frequency and loss factor) of composite specimens were determined prior to applying or subjecting the specimens to a static pre-load. The loss factor and resonant frequency were used in Equation (2) and Equation (3) to predict the joint shear strength, and thus the failure load.

Based on the estimated or predicted fracture load, load levels equal to 25%, 50% and 75% of the failure were chosen. Selected composite specimens were subjected to a static pre-load of 25% of the estimated or predicted fracture load. The load was applied for a period of 30 minutes. At the end of this time period, the composite specimens were removed from the MTS machine, and subjected to flexural vibration test to ascertain if the static pre-load had induced any

damage, which would be evident through changes in resonant frequency and damping (loss factor). Following the non-destructive flexural vibration test, the samples were re-loaded in the MTS machine to a load level of 50% of the predicted fracture load, for a time period of 30 minutes. This was followed by dynamic testing to detect damage or degradation of the adhesive joint. The specimens were then loaded to a level of 75% of the estimated fracture load, and non-destructively tested to detect damage. The composite specimens were finally loaded to failure (defined as relative separation of the 'male' adherend from the 'female' adherend due to failure of the adhesive).

Results documented in Table 6 reveal no appreciable change in damping (Figure 38) or resonant frequency (Figure 39) as a result of subjecting the adhesively joined specimens to a static preload. The results indicate a failure of the pre-load levels chosen to induce any significant or appreciable damage such as debond or adhesive cracking that could serve as potential sites for promoting catastrophic crack propagation. The load levels were apparently well within the elastic limit and failed to cause any appreciable deformation in the adhesive. This observation is well substantiated by the load-displacement curve resulting from a tensile test conducted on bulk (dog-bone specimens) Epon 815 epoxy (Figure 40). The epoxy material exhibits non-linearity just prior to fracture.

The authors believe that in order to cause any

appreciable damage in the epoxy chosen, the load level must be adequate to cause plastic deformation in the adhesive, and/or the load regardless of its magnitude, should be applied for a substantial period of time (could result in viscoelastic creep in the adhesive) in order to induce damage. Alternatively, repeated loading or cyclic plastic deformation could be used to initiate and grow fatigue cracks.

The actual fracture load of the composite specimens after subjecting them to static pre-loads, agreed well with the value estimated by using Equation (2) and Equation (3). This correlation proves the accuracy of the equations describing the curves (Figures 36 and 37) that best fit the variation of dynamic properties with joint shear strength for different type, degree and severity of defects.

In order to evaluate the effect of loading on joint durability, additional study needs to be done at load levels in the plastic regime of the epoxy used, and/or load levels applied for time periods greater than the one chosen (30 minutes) in this study, and/or cyclic loading.

12. DEFECT QUANTIFICATION AND ANALYSIS

The effect of porosity was measured by preparing the adhesive joint specimens with the adhesive mixture (epoxy EPON 815 and Hardener V-40) degassed prior to casting, for time periods of 0, 2 and 7 minutes. Previous work has shown

[10,11] that degassing for 7 minutes reduces the porosity to negligible proportions. Omission of the degassing step usually results in the development of fine microscopic pores during curing. Damping measurements were made on the resulting adhesively joined specimens, which were eventually pulled to failure in a universal testing machine, at a crosshead speed of 0.2 in/min. The variation of damping (loss factor) and strength (shear strength) with adhesive degassing time is exemplified in Figure 41. It is observed that no degassing of the adhesive mixture, i.e., case of 0 minutes degassing, results in degradation in strength and increased damping.

The separated joints (separation of the 'male' adherend from the 'female' adherend) were first examined under a low power stereomicroscope. A few pores were observed on the surface and embedded in the epoxy of specimens that was not degassed, while none were observed in specimens in which the adhesive mixture was degassed for time periods of 2 and 7 minutes. The clevises were carefully sawn off the specimens, to produce roughly square steel specimens with the adhesive still attached. The 0 minute degassed specimens failed predominantly by interfacial shear, while the specimens in which the adhesive was degassed for 2 and 7 minutes, failed partly by interfacial shear and partly by tensile fracture of the adhesive. The fractured specimens were gold-coated in a vacuum deposition chamber, and the interfacial adhesive and

the fracture surface of the adhesive examined in a scanning electron microscope. The fractures were brittle, and showed evidence of extensive mirror and hackle (river pattern) regions. A few pores were found on the fracture surfaces, but none were found at expected origins. The interfacial failure surfaces imaged the machining patterns on the surface of the steel. Very few microscopic pores were found in the specimen whose adhesive mixture was not degassed (0 minute degassing). Typical areas were photographed at a magnification of x250. A typical view of the surface is shown in Figure 42. An extensive survey of the interfaces of the specimens in which the adhesive was degassed for 2 minutes and 7 minutes, revealed only one isolated group of pores. In the vast majority of areas, no pores were observed. This is shown in the electron micrograph in Figure 43.

Since the joints failed mainly by interfacial separation, it was expected that the pores at an interface would affect strength. Damping should be influenced by pores both at the surface and those embedded in the adhesive. This hypothesis was born out by the results obtained in this study. It seems plausible that the reaction kinetics betwen the EPON 815 epoxy and the hardener is different when the adhesive mixture is not degassed under vacuum when compared to the strong reaction accompanied by the evolution of gas bubbles that occurs when degassed under vacuum (Figure 13). The change in reaction kinetics could be an additional factor

contributing to the observed differences in damping and strength.

The 0 minute degassed specimens show markedly different strength and damping in comparison to those that were degassed for 2 minutes and 7 minutes. Yet, SEM observations revealed the presence of very few microscopic pores in the 0 minute degassed specimens. It appears that both joint strength and damping are very sensitive to: (i) porosity, (ii) changes in reaction kinetics of the adhesive mixture, and (iii) chemistry of the adhesive. This sensitivity needs to be confirmed by more extensive testing and analysis. Regardless of the need for additional quantification, it is certain that the impulse hammer technique gives a sensitive measure of the presence of fine microscopic defects such as pores, changes in reaction kinetics and adhesive chemistry.

13. SUMMARY AND CONCLUDING REMARKS

- In this Phase I investigation, inherent flaws such as: (i) local regions of poor cure, (ii) porosity, (iii) voids, and (iv) disbonds caused by poor surface preparation and by impurities on the adhesive-adherend interface, were created in the adhesive joint of composite specimens (two steel adherends held together by a double-lap adhesive joint) through careful control of processing variables.
- The impulse-frequency response technique successfully

detects the presence of both macroscopic (debond) and microscopic (pores) flaws as is reflected by a pronounced increase in damping (loss factor) with an increase in size, number and severity of the flaws.

- The presence of both macroscopic and microscopic flaws results in a degradation in the shear strength of the adhesive joint.
- The observed change in damping (loss factor) with cure time at the accelerated cure temperature is attributed to several competing mechanistic processes involving:
  (a) shrinkage of the adhesive,
  (b) chemical and physical characteristics of the adhesive relative to the adherend, and
  (c) thermal stresses.
- A level of fine microscopic pores and a few macroscopic voids were induced by not degassing the adhesive mixture. The pores and voids coupled with changes in the reaction kinetics of the adhesive mixture causes a large change in damping which is detected by the impulse-frequency response technique. The internal pores affect damping while those at an interface cause a marked degradation in adhesive joint strength, besides contributing to damping changes.
- Debond areas within an adhesive joint were observed to cause a marked increase in damping with concomitant reduction in strength of the adhesive joint. The damping was observed to increase exponentially with an increase

in debond area. The increase in damping was found to correlate well with degradation in strength of the adhesive joint.

- For different types, degree and intrinsic severity of flaws, a relationship has been developed to predict strength of an adhesive joint from its dynamic properties (loss factor and resonant frequency). The actual fracture strength or load accords reasonably well with the predicted value obtained using this relationship.
- Loading the adhesive joint specimens to levels in the elastic range of the epoxy, and for short time-periods, was found to be inadequate to induce any appreciable damage in the adhesive or corresponding changes in damping.
- Results of this study have shown conclusively that the impulse technique has considerable potential for non-destructive evaluation of the structural integrity of adhesive joints.

REFERENCES

1. E. A. Huntress: A. M. Mach., Special Report-716, pp. 145-160, October 1979.

2. E. M. Petric: Adhesives Age, Vol. 23, 1980, pp. 14-23.

3. M. M. Villalobos and P. Czarnock: J. Adhesion, Vol. 19, 1986, pp. 79-87.

4. R. W. Shannon:"Primary Adhesively Bonded Structure Technology", AFFDL-TR-77-107, Air Force Flight Developoment Laboratory, Dayton, Ohio, September 1977.

5. R. Mantena, T. A. Place and R. F. Gibson: "Characterization of Matrix Cracking in Composite Laminates by the Use of Damping Capacity Measurements," Symposium on Role of Interfaces on Material Damping, TMS-AIME Fall Meeting, Toronto, Canada, October 1985, ASM Paper No. 8522-002.

6. R. D. Adams and N. A. Peppiatt: J. Strain Analysis, Vol. 9, 1974, pp. 185-196.

7. R. D. Adams amd W. C. Wake: Structural Adhesive Joints in Engineering, Elsevier Applied Science Publishers, 1984, pp. 133-137.

8. S. A. Suarez and R. F. Gibson:"Computer Aided Dynamic Testing of Composite Materials," Proceedings of the Fall 1984 Meeting of the Society of Experimental Mechanics, Milwaukee, Wisconsin, 1984.

9. S. A. Suarez and R. F. Gibson: J. of Testing and Evaluation, Vol. 15(2), 1987, pp. 114-121.

10. S. Gunawan and R. F. Gibson: "Analytical and Experimental Characterization of Extensional Damping in Single Lap Viscoelastic Adhesive Joints," AIAA/ASME/ASCE/AHS 28th Structures, Structural Dynamics and Materials Conference, Paper No. AIAA-87-0886-CP, Monterey, CA, April 6-8, 1987.

11. S. Gunawan: "Damping Characteristics of the Single-Lap Adhesive Joint using Finite Element and Extensional Vibration Analysis," Master of Science Thesis, Dept. of Mechanical Engineering, University of Idaho, April 1986.

12. R. T. Thompson: "Design Considerations for Adhesively Bonded Plastic Joints," AD85-776, Society of Manufacturing Engineers.

13. K. W. Allen and H. S. Alsalim: J. Adhesion, Vol. 8, 1977, pp. 183-194.

14. G. L. Schneberger: Adhesives Age, 1985, pp. 18-20.

15. E. Sancaktar, H. JoZavi and R. M. Klein: J. Adhesion, Vol. 15, 1983, pp. 241-251.

16. R. W. Hylands and E. H. Sidwell: J. Adhesion, Vol. 11, 1980, pp. 203-218.

17. R. O. Ebewele, B. H. River and J. A. Koutsky: J. Adhesion, Vol. 14, 1982, pp. 189-217.

TABLE 1

Stiffness Properties of the EPON 815 Epoxy

(a) Storage Modulus = 0.310×10^6 psi = 2.137 GPa (Dynamic-Flexure)

(b) Static Modulus = 0.244×10^6 psi = 1.682 GPa (Bending)

(c) Static Modulus = 0.304×10^6 psi = 2.096 GPa (Tension)

Table 2

Dimensions of Composite Test Specimens and Test Conditions

(a)	Length of composite specimen	= 101.60 mm
(b)	Width of the composite specimen	= 19.05 mm
(c)	Adherend thickness	= 3.56 mm
(d)	Adhesive thickness	= 0.056 mm
(e)	Density of Steel	= 7.76 g/cm^3
(f)	Yield strength of steel	= 379 MPa
(g)	Tensile Strength of Steel	= 571 MPa
(h)	Density of epoxy (EPON 815)	= 1.085 g/cm^3
(i)	Test Temperature	= 70-80 F
(j)	Humidity	= 55-65 percent

TABLE 3.

Effect of Curing Time on Loss Factor*, Resonant Frequency#, and Strength+.

Cure-time (minutes)	Loss Factor	Percentage change in loss factor	Resonant Frequency (Hz)	Percentage change in Resonant Frequency	Shear Strength (psi)	Percentage change in shear strength
240	0.0192	-	261.70	-	2167	-
180	0.0197	+2.60	268.40	+2.56	2800	+29.20
120	0.0184	-4.10	268.90	+2.75	2767	+27.68
60	0.0259	+35.00	261.50	-0.08	967	-55.30

*, # results are the mean based on three tests, and each test is the average of four trials.

\+ results are the mean of two tests.

Table 4.

Effect of Degassing time on Loss Factor*, Resonant Frequency+, and Strength#.

Adhesive Degassing Time (minutes)	Loss Factor (η)	Percentage change in Loss Factor	Resonant Frequency (Hz)	Percentage change in Resonant Frequency	Shear Strength (psi)	Percentage change in shear strength
7	0.02531	-	267.028	-	1517.0	-
2	0.0225	-10.90	265.256	-0.66	2566.5	+69.20
0	0.1380	+445.00	191.515	-28.28	373.5	-75.37

*,+ results are the mean based on three tests, and each test is the average of four trials.

\# results are the mean of two tests.

TABLE 5.

Effect of Debond Area on Loss Factor*, Resonant Frequency+, and Strength#.

Debond Area (%)	Loss factor (η)	Percentage change in loss factor	Resonant Frequency (Hz)	Percentage change in Resonant Frequency	Shear Strength (psi)	Percentage change in Shear Strength
0	0.0183	-	265.34	-	2950.0	-
25	0.0590	+222.40	174.70	-34.16	883.0	-70.06
50	0.0770	+320.76	223.80	-15.66	1883.0	-36.17
75	0.3650	+1894.54	67.53	-74.55	193.0	-93.45

*,+ results are the mean based on three tests, and each test is the average of four trials.

results are the mean of two tests.

Table 6.

EFFECT OF PRE-LOADING ON LOSS FACTOR* AND RESONANT FREQUENCY

Load Condition	Loss Factor	Percentage Change in Loss Factor	Resonant Frequency (Hz)	Percentage Change in Resonant Frequency
No Pre-loading	0.0198	-	261.61	-
1000 lbs	0.0208	+5.05	258.92	-1.02
2000 lbs	0.0212	+7.07	260.67	-0.36
3000 lbs	0.0216	+9.09	256.91	-1.80

*, # results are the mean based on three tests, and each test is the average of four trials.

Table 7.

EFFECT OF PRE-LOADING ON FRACTURE

Specimen No.	Condition	Estimated* Fracture Load (lbs)	Actual Fracture Load (lbs)	Percentage Change in Estimated Fracture Load
L-39	No Pre-load	3600	3500	-3.0
L-40	Preloaded to (a) 1000 lbs for 30 min. (b) 2000 lbs for 30 min. (c) 3000 lbs for 30 min	3900	3450	-12.0
L-41	Preloaded to (a) 1000 lbs for 30 min. (b) 2000 lbs for 30 min. (c) 3000 lbs for 30 min.	3500	3100	-11.0
L-42	Preloaded to (a) 1000 lbs for 30 min (b) 2000 lbs for 30 min (c) 3000 lbs for 30 min.	3700	3750	+1.0

* average value of Equations (2) and (3).

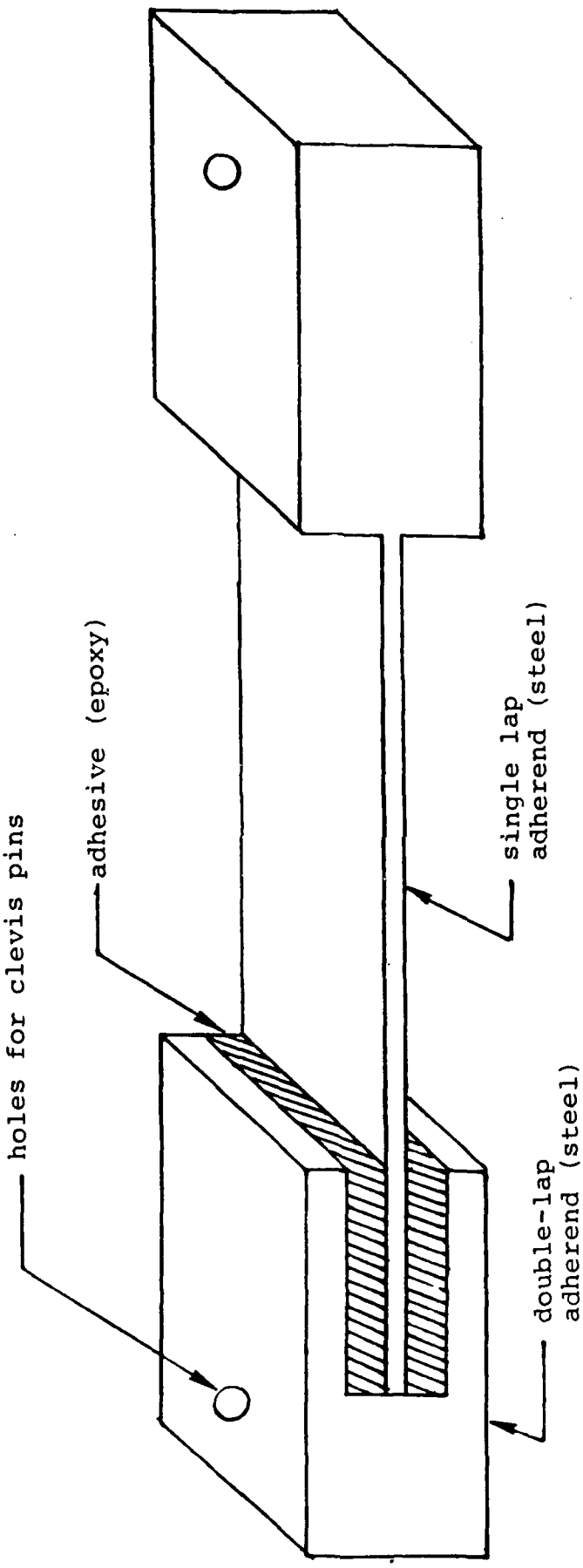

Figure 1. Schematic showing configuration of the composite test specimen.

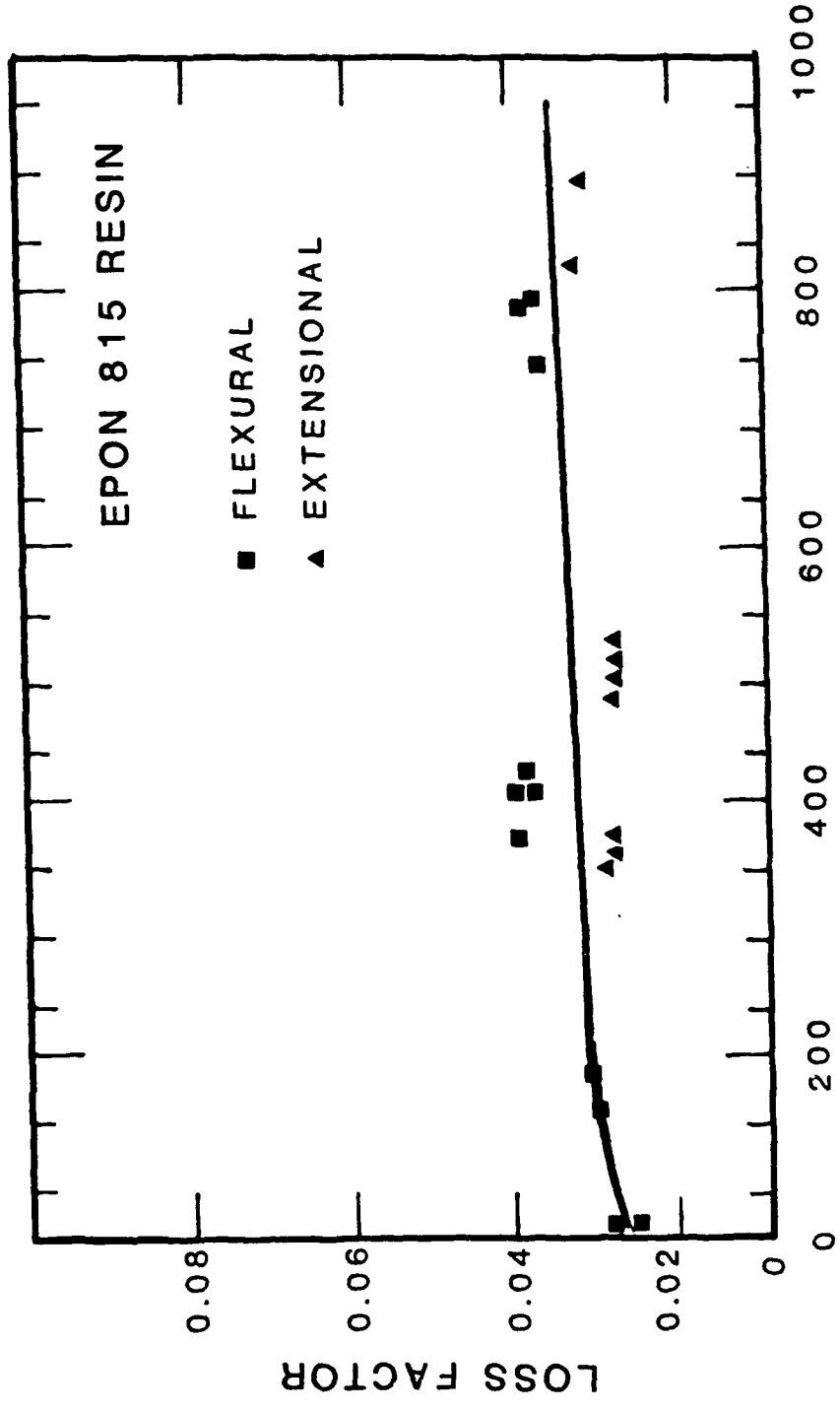

Figure 2. Variation of loss factor with frequency (Hz) for the EPON 815 resin.

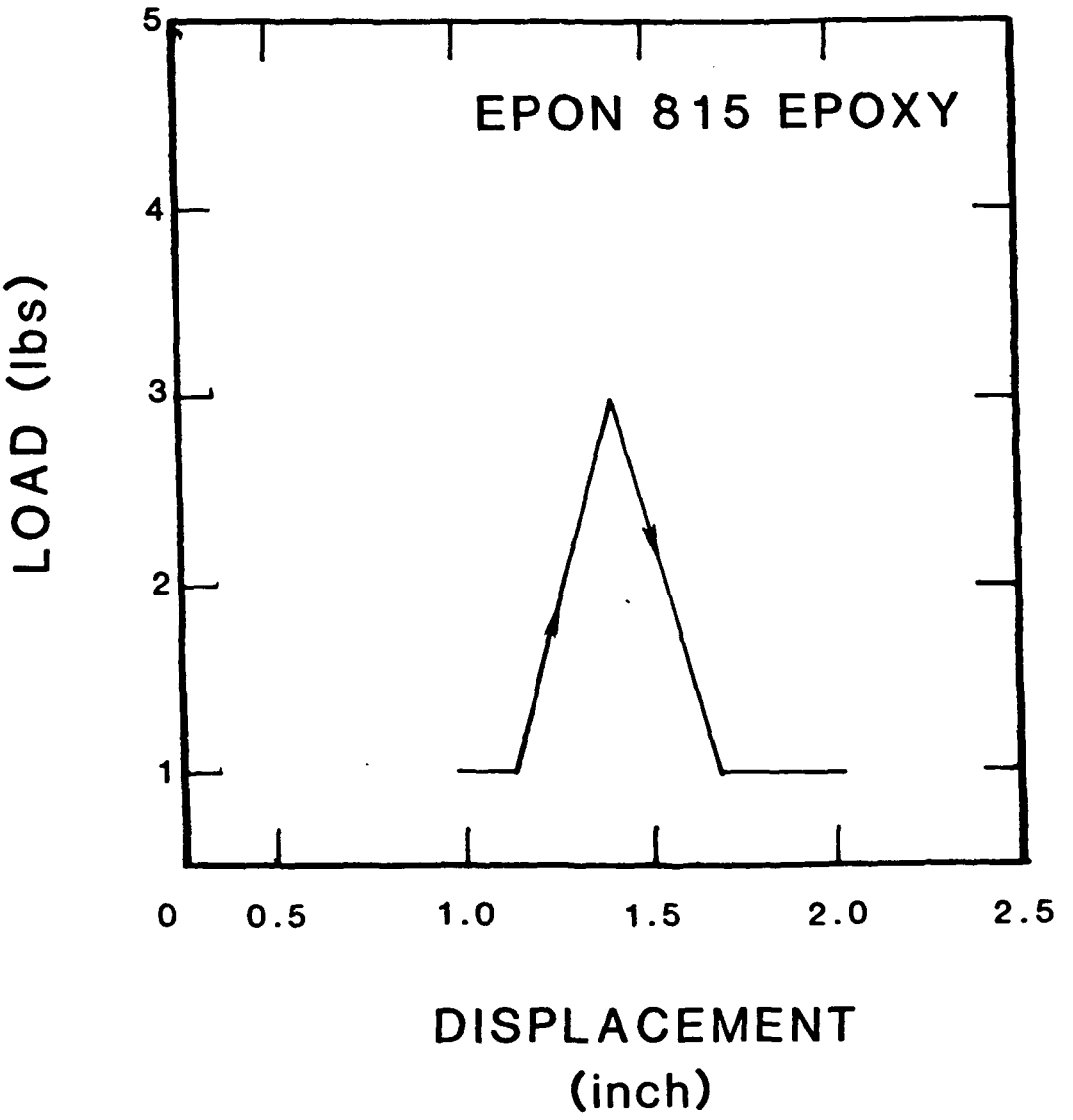

Figure 3. Load-Displacement curve obtained for the EPON 815 epoxy from a three-point bend test.

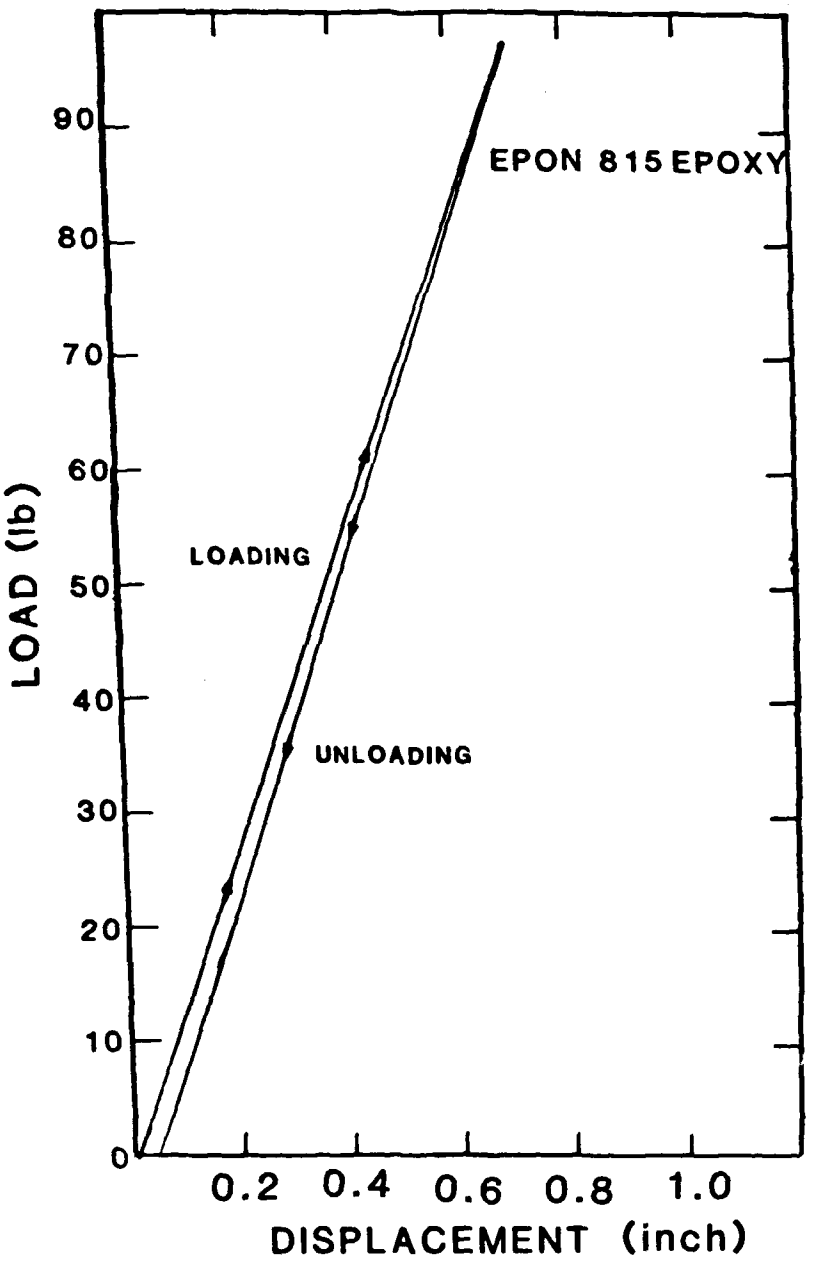

Figure 4. Load-Displacement curve for the EPON 815 epoxy, from a uniaxial tensile test.

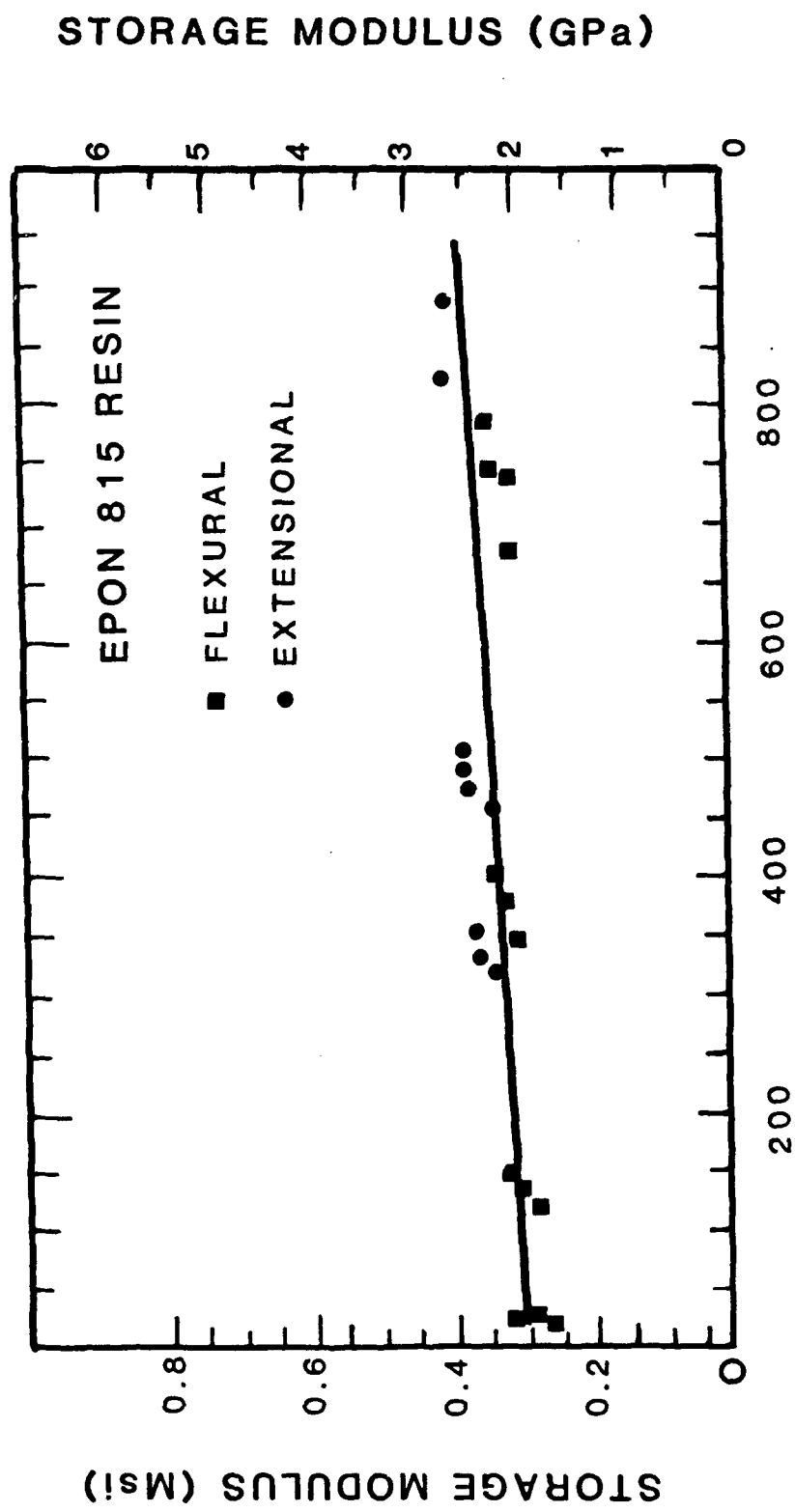

Figure 5. Variation of dynamic modulus with frequency for the EPON 815 resin.

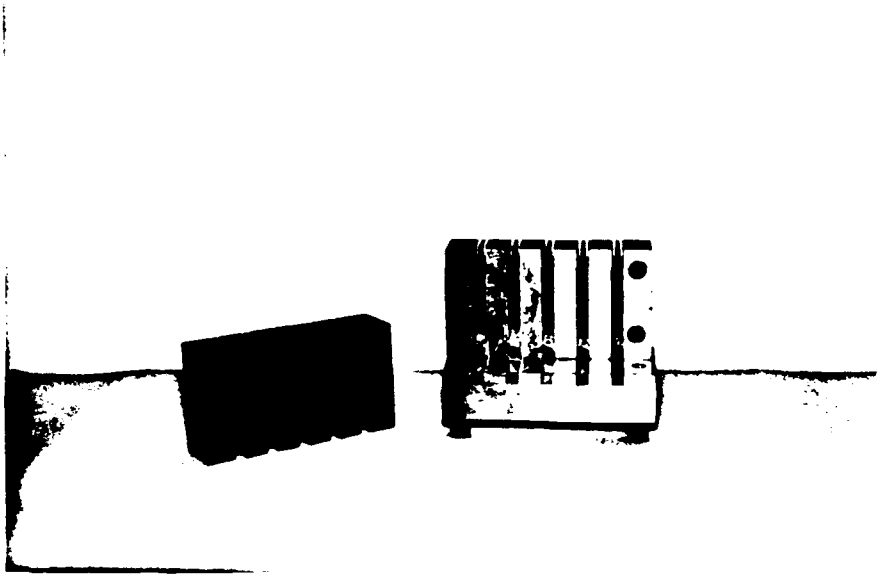

Figure 6. Split-die mounted on the base plate of the alignment jig with provisions for accommodating five test specimens.

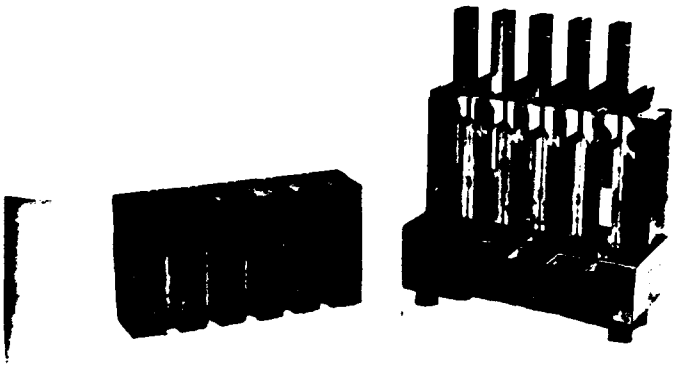

Figure 7. Section through the alignment jig showing positioning of the adhesively bonded test specimens.

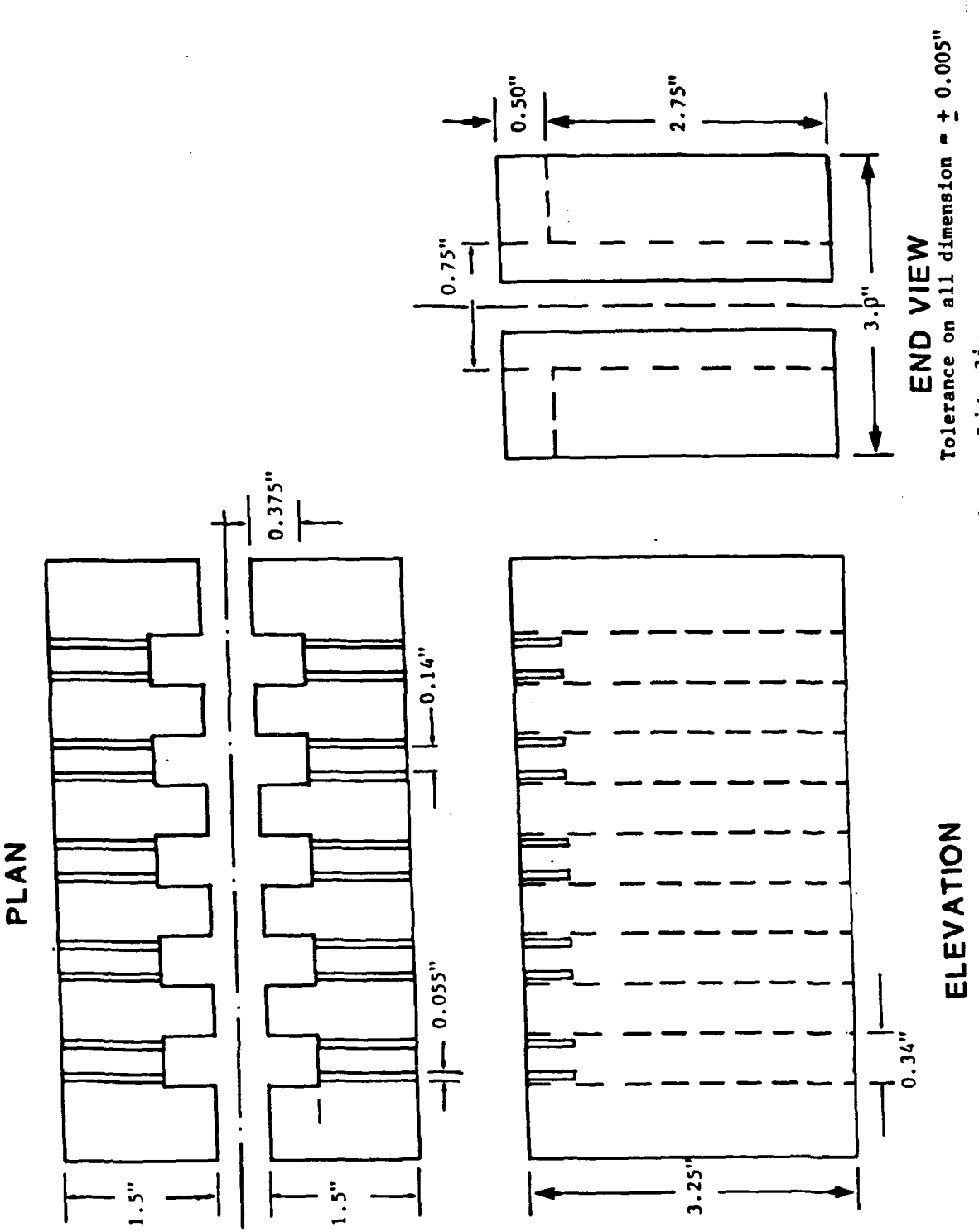

Figure 8. Schematic showing dimensions of the split-die.

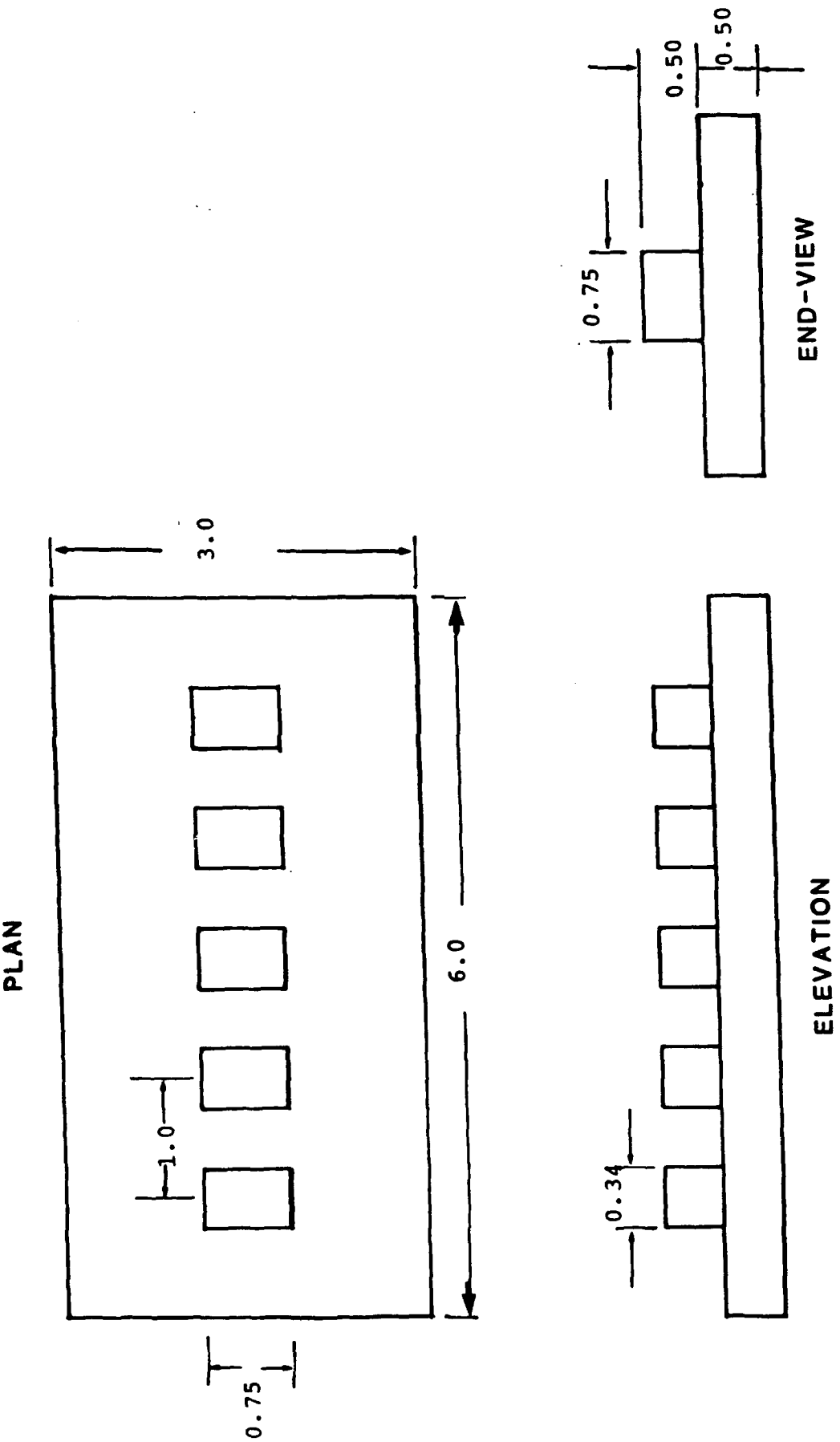

Figure 9. Schematic showing dimensions of the base-plate.

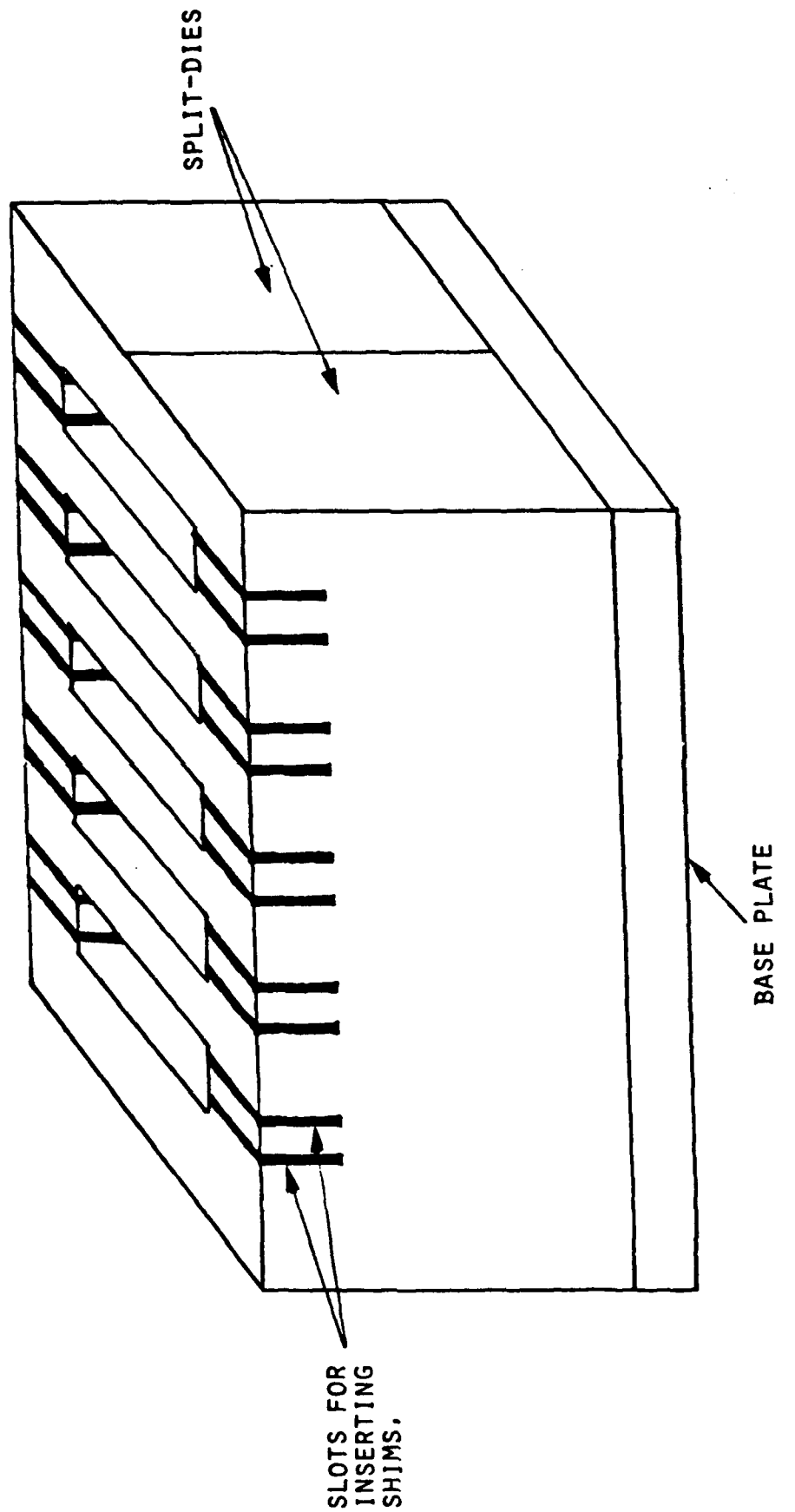

Figure 10. Typical view of assembled jig for the adhesively joined steel specimen.

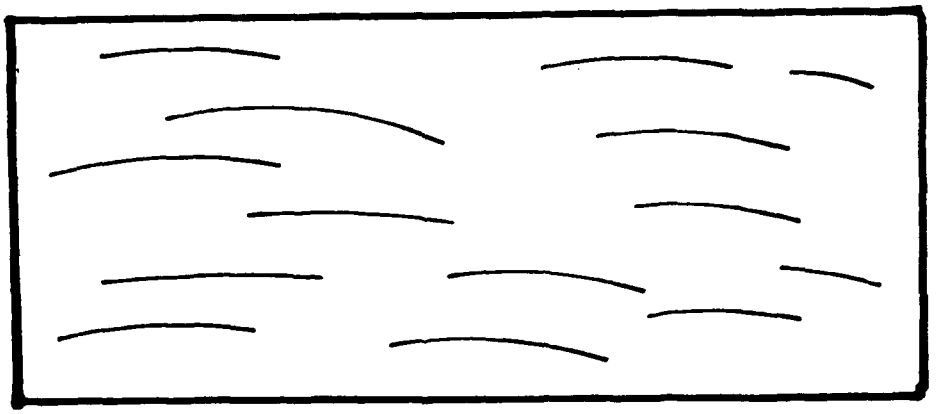

CLEAN SURFACE

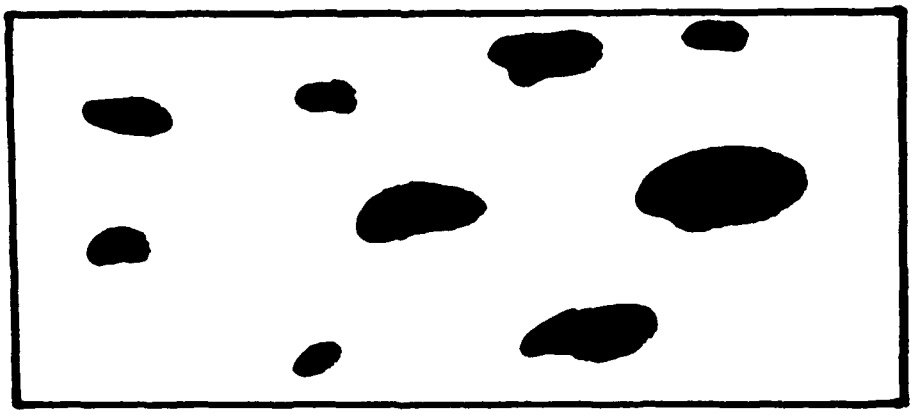

DIRTY SURFACE

Figure 11. Schematic showing water forming a film on a clean surface, and droplets on a dirty surface.

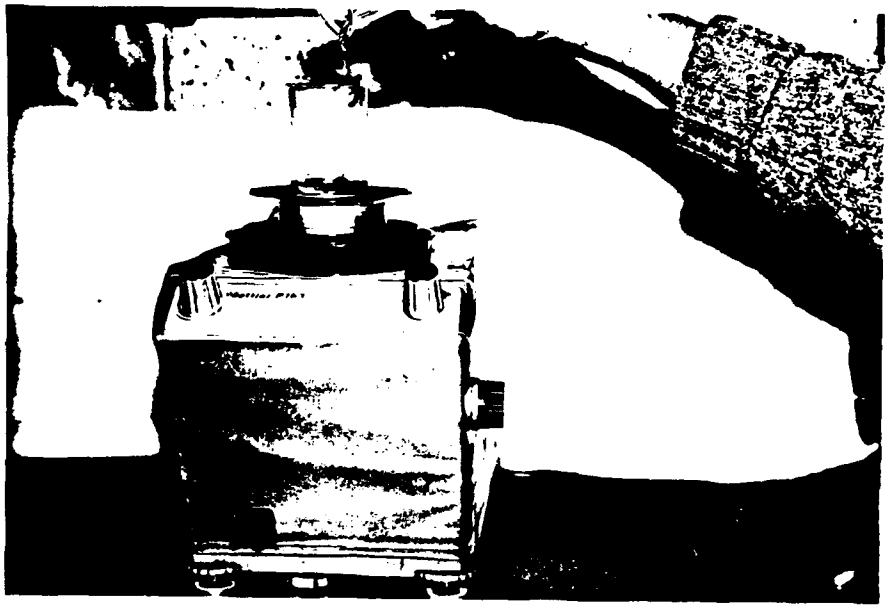

Figure 12. Weight measurements being made on a Mettler balance.

Figure 13. Mixture of epoxy and hardener being degassed under vacuum at a temperature of 100 C (212 F).

Figure 14. Viscous adhesive being poured into the 'female' adherend of the double-lap test specimen.

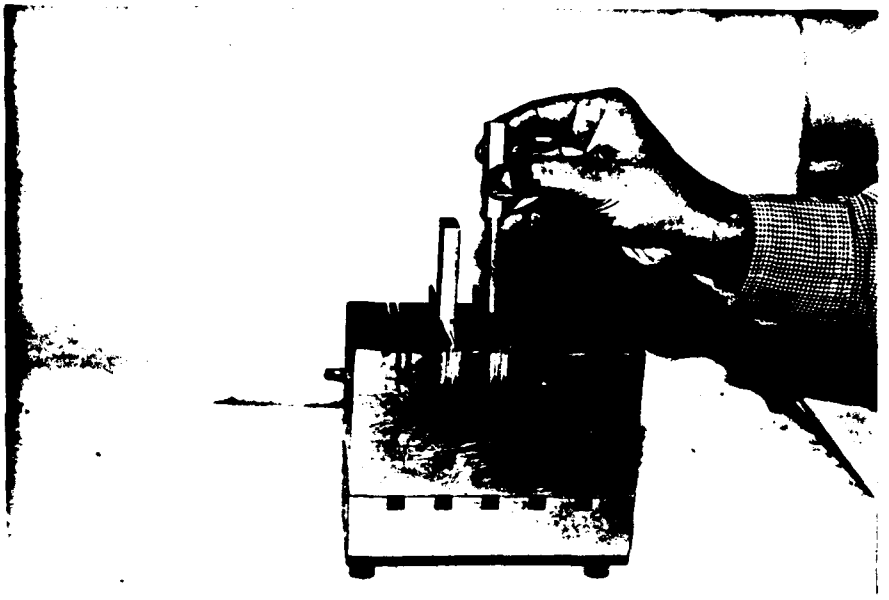

Figure 15. The 'male' adherend being lowered into the double-lap 'female' adherend.

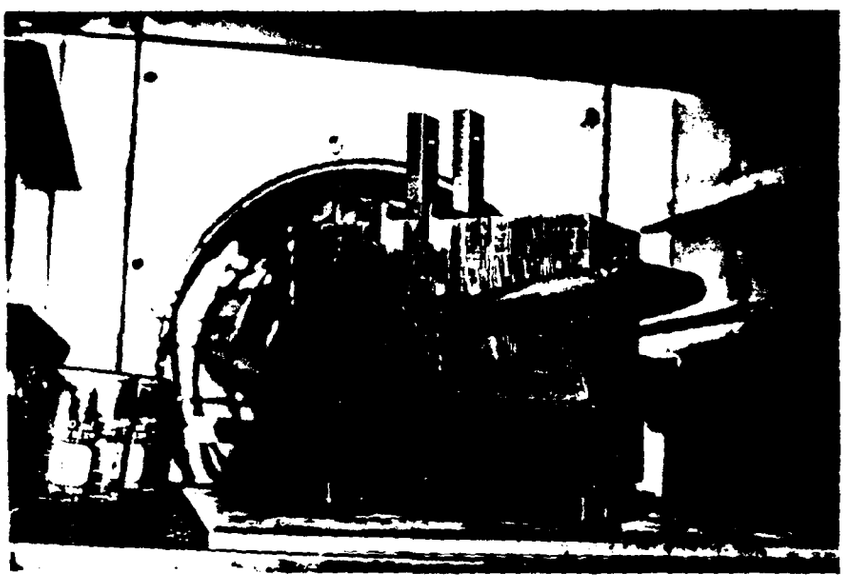

Figure 16. Assembled jig with specimen in position, placed in an oven for curing of the adhesive.

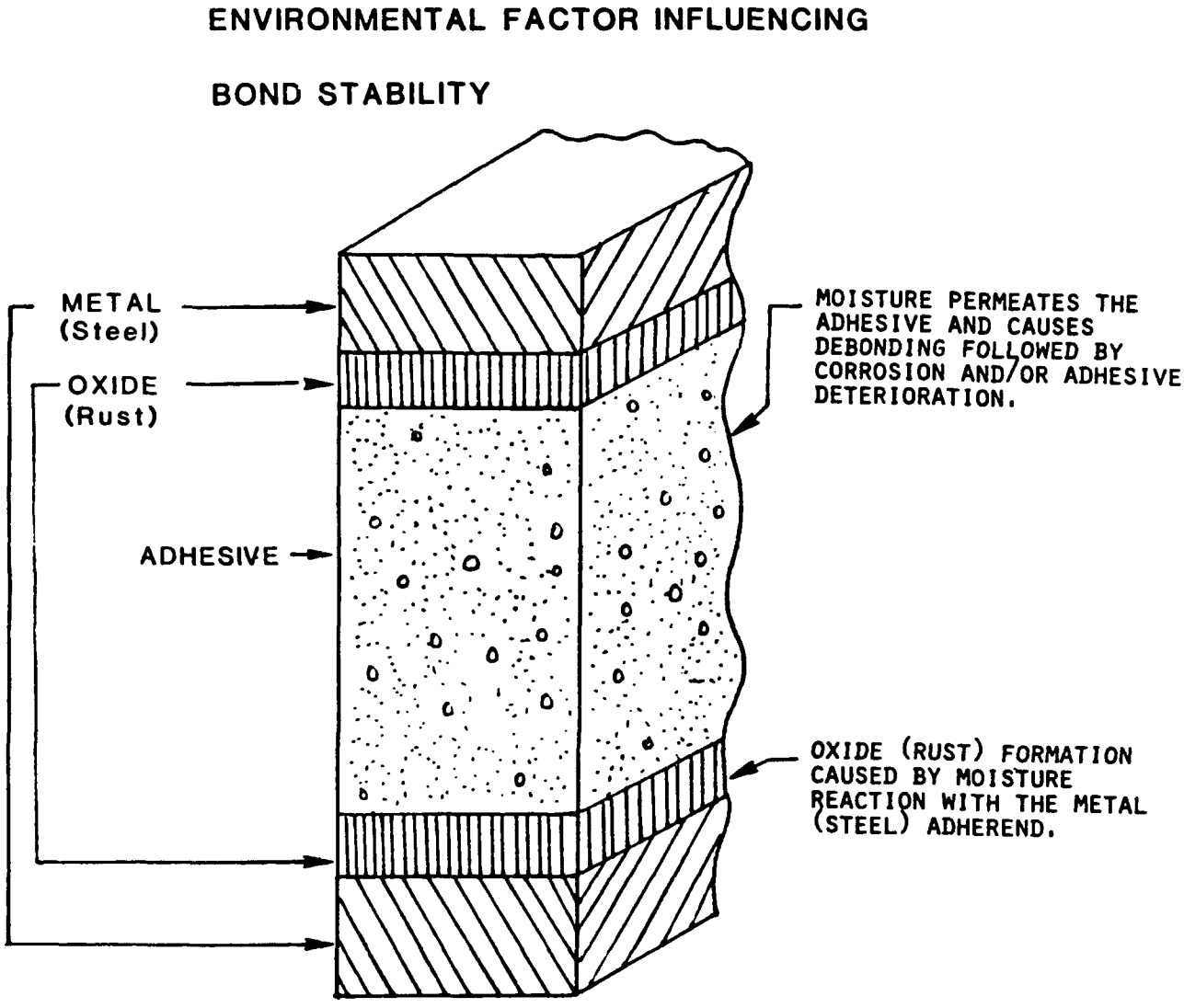

Figure 17. Environmental effect on adhesive bond durability.

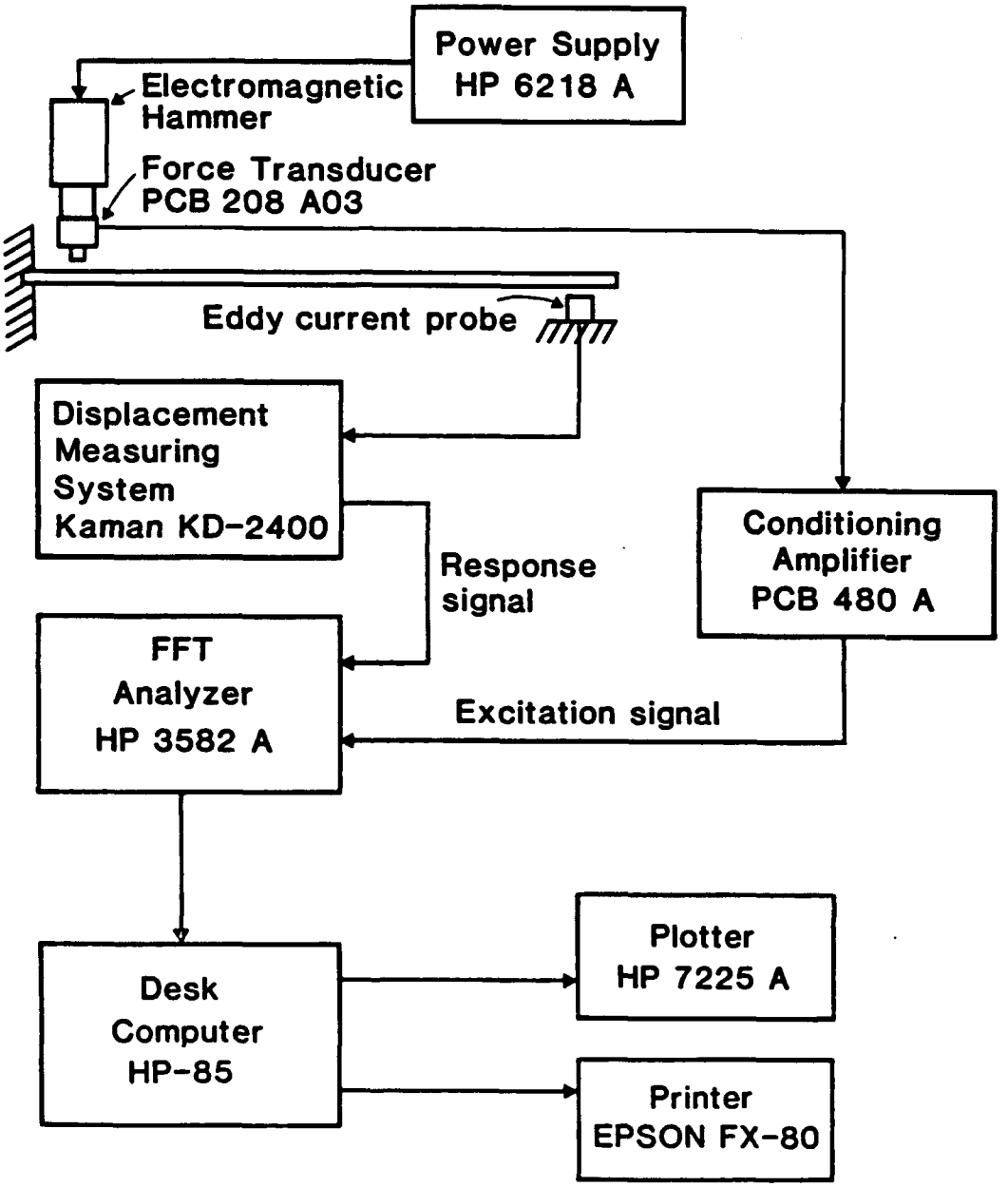

Figure 18. Block diagram showing the flexural vibration apparatus.(Ref.8,9).

LOGARITHMIC SCALE = AT 3 dB BELOW THE PEAK VALUE (AT RESONANT FREQUENCY)

LINEAR SCALE = AT 0.707 THE PEAK VALUE

LOSS FACTOR = $\frac{\Delta f_n}{f_n}$

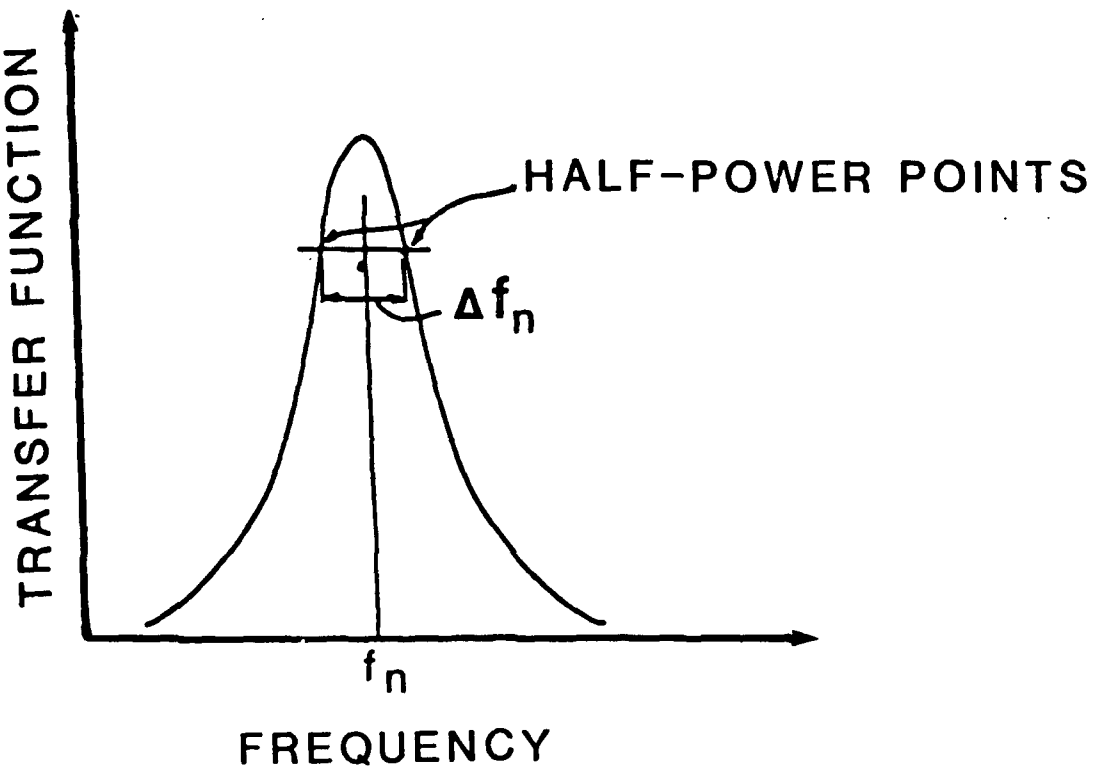

Figure 19. The half-power bandwidth.

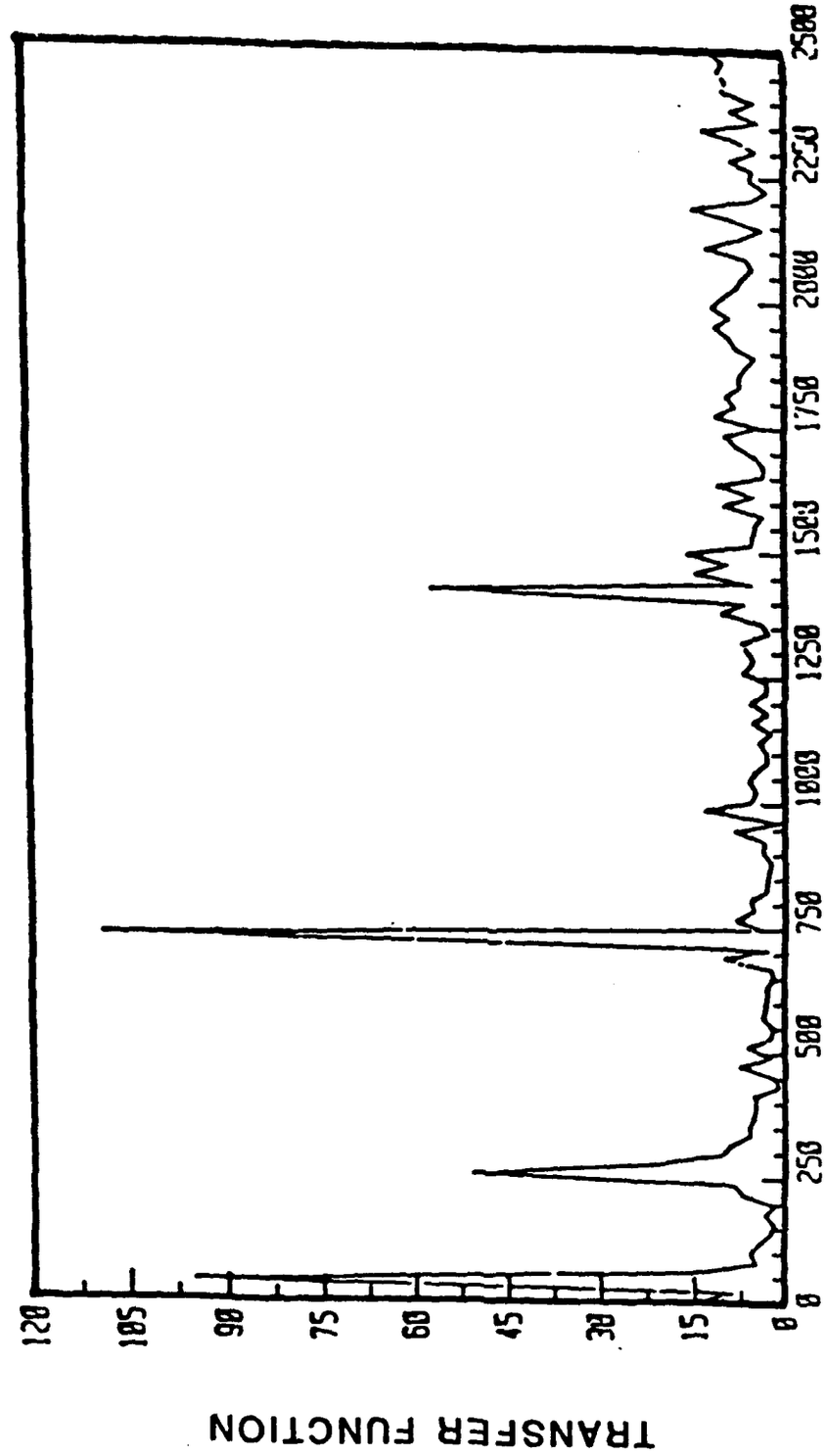

Figure 20. Typical transfer function trace on screen on the Fast Fourier Transform (FFT) analyzer.

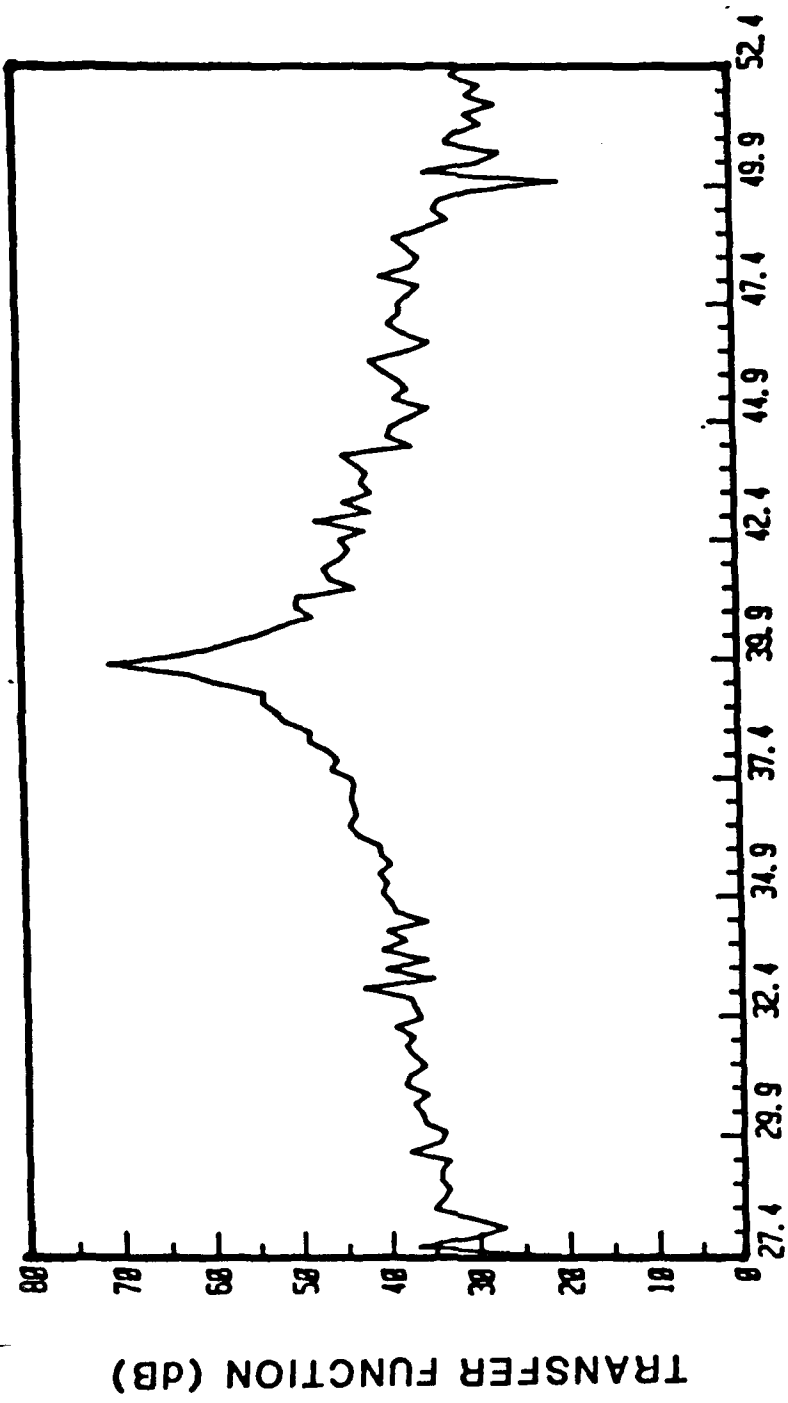

Figure 21. Peak of transfer function at one mode using "zoom" feature on the Fast Fourier Transform (FFT) analyzer.

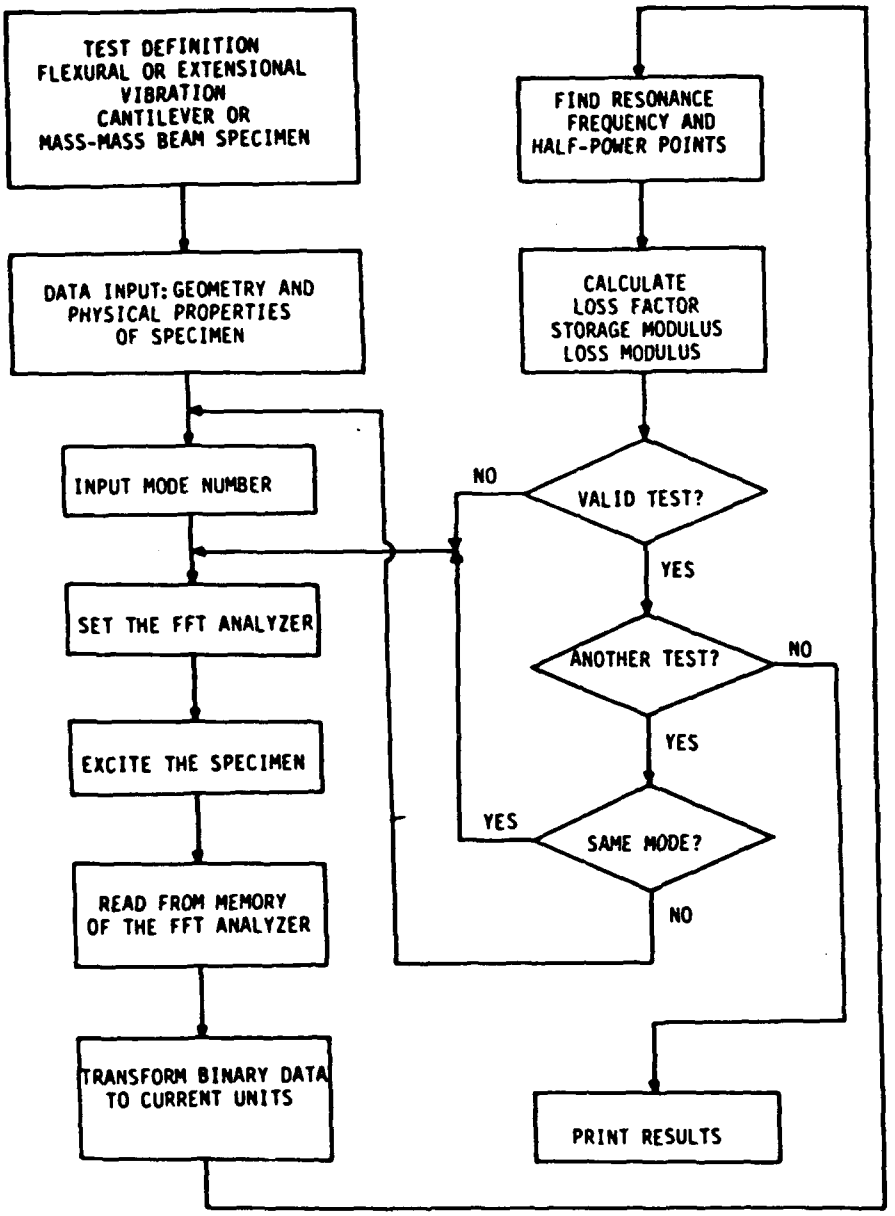

Figure 22. Flow chart for data acquisition and reduction program (Ref. 8,9).

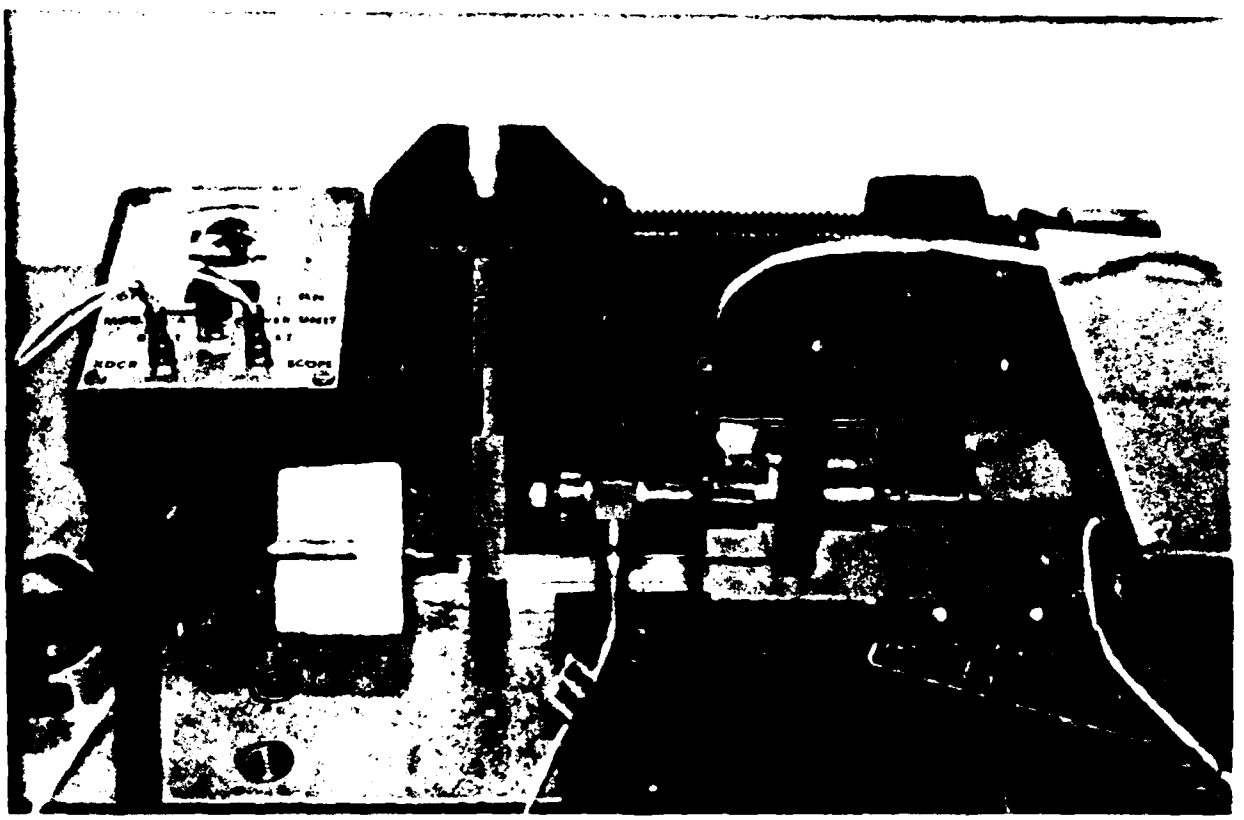

Figure 23. Test set-up for the flexural vibration test, showing relative position of the impulse hammer and non-contacting eddy current probe with reference to the adhesively joined specimen (fixed-free end condition).

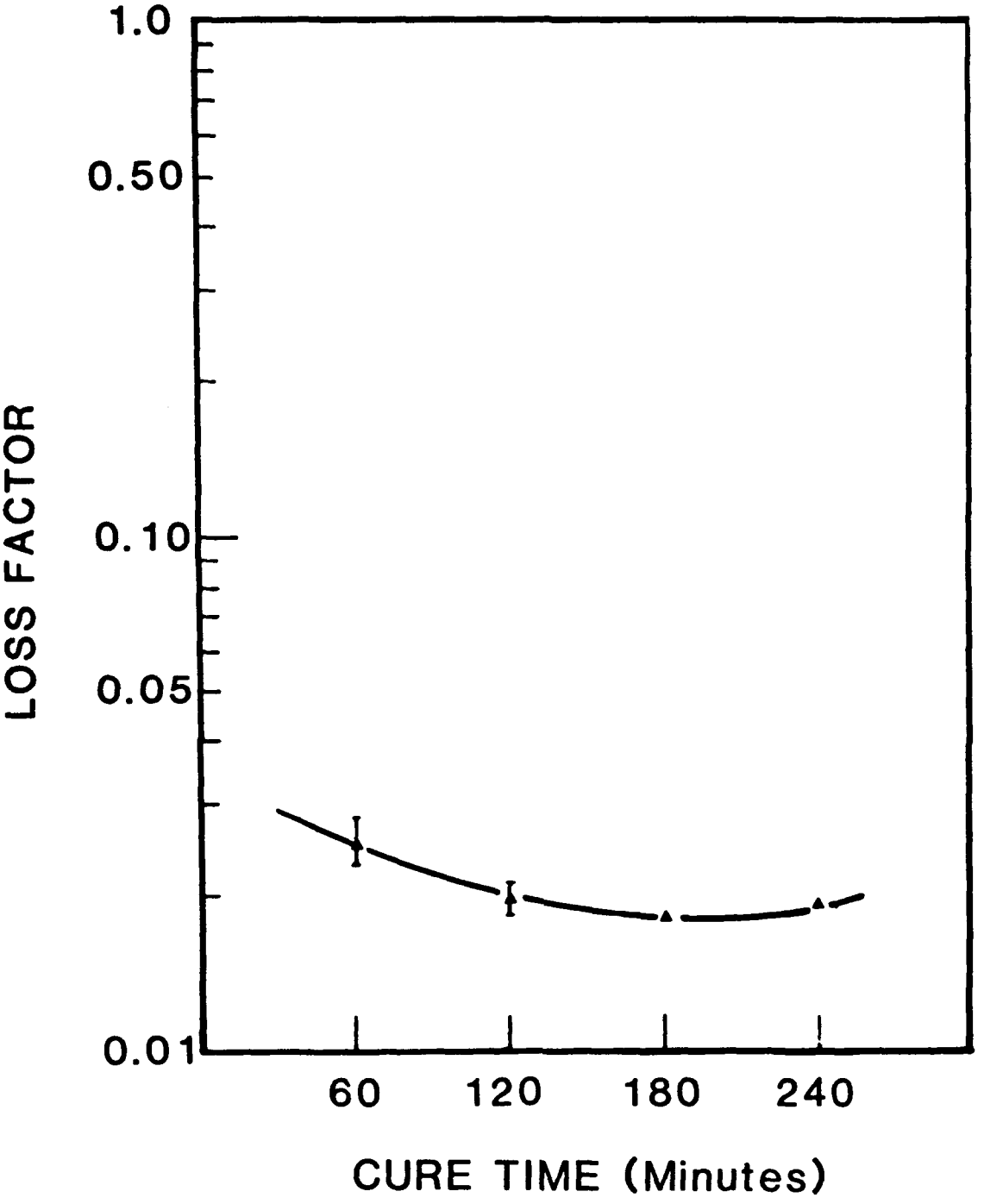

Figure 24. Effect of accelerated cure time (minutes) on damping of adhesive joint.

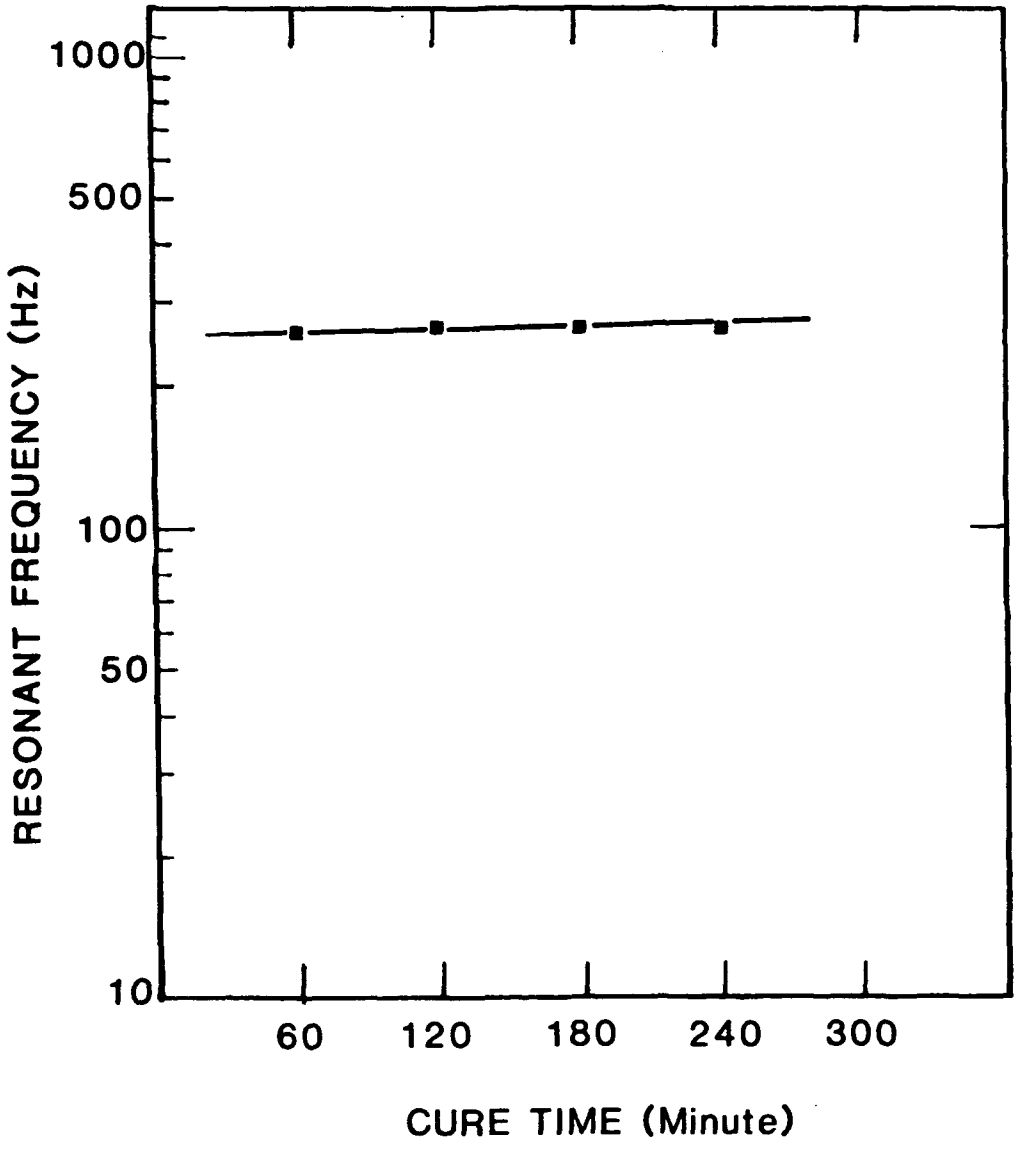

Figure 25. Variation of 1st Mode resonant frequency (Hz) of adhesive joint with cure time (minutes).

Figure 26. Set-up on MTS machine showing clip-gage extensometer fixed to the composite specimen at the double-lap adhesive joint end.

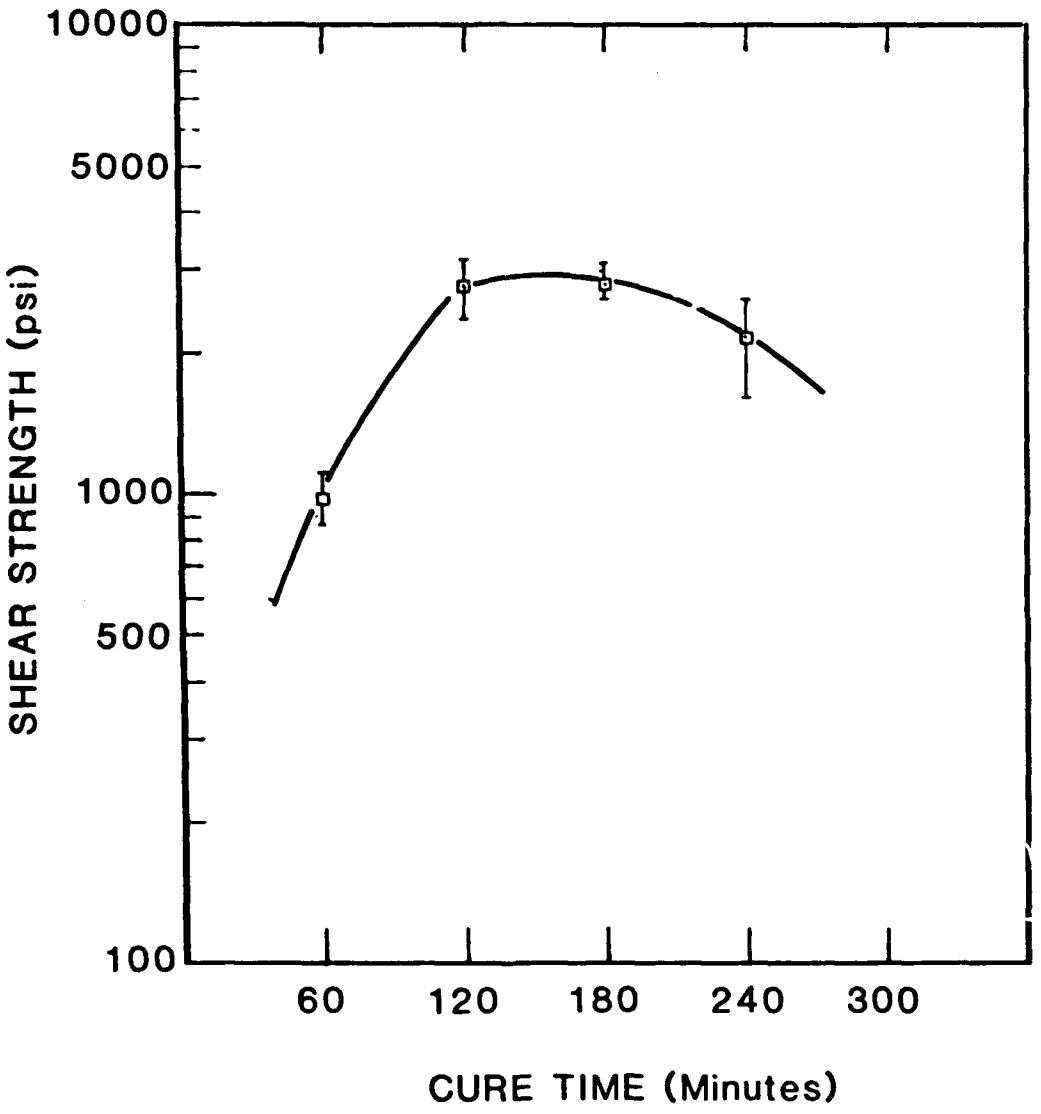

Figure 27. Variation of joint shear strength (psi) with cure time (minutes).

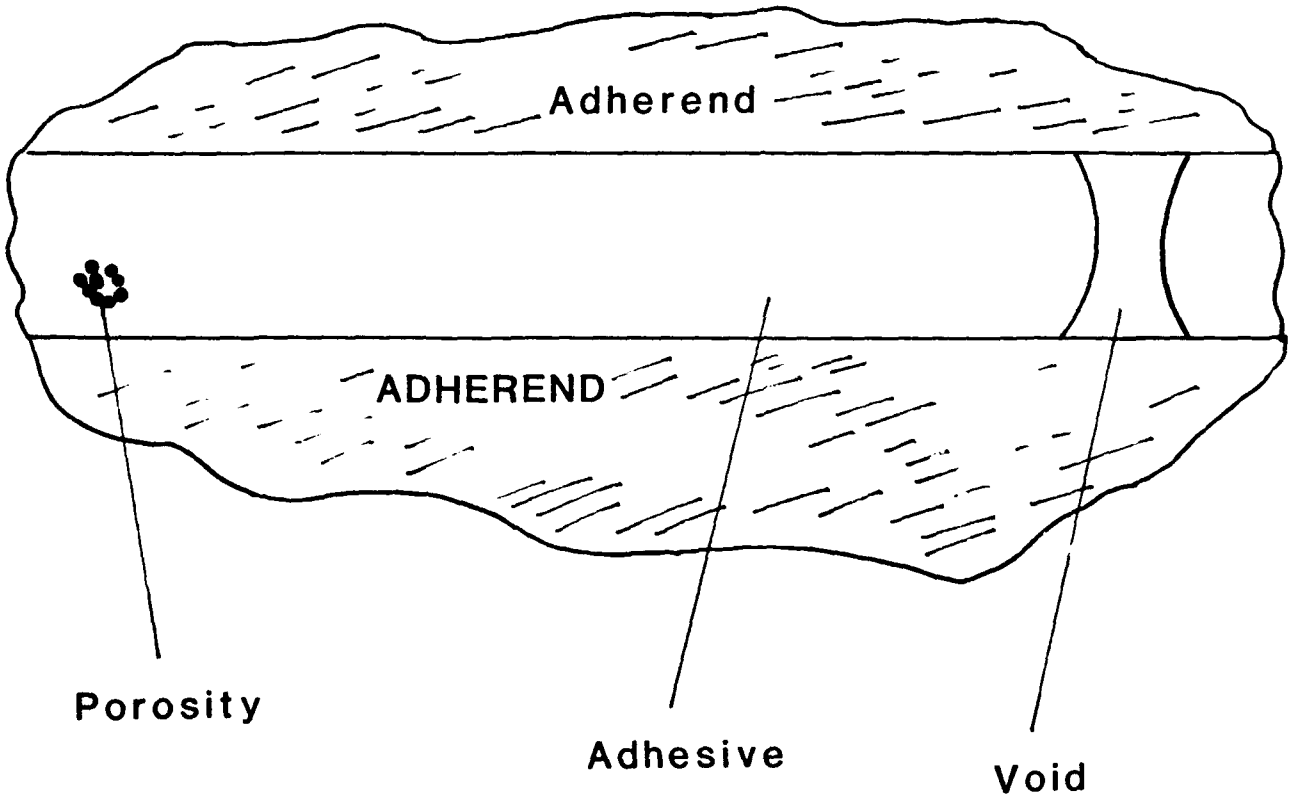

Figure 28. Typical defects: porosity and voids, caused by entrapped air in the adhesive.

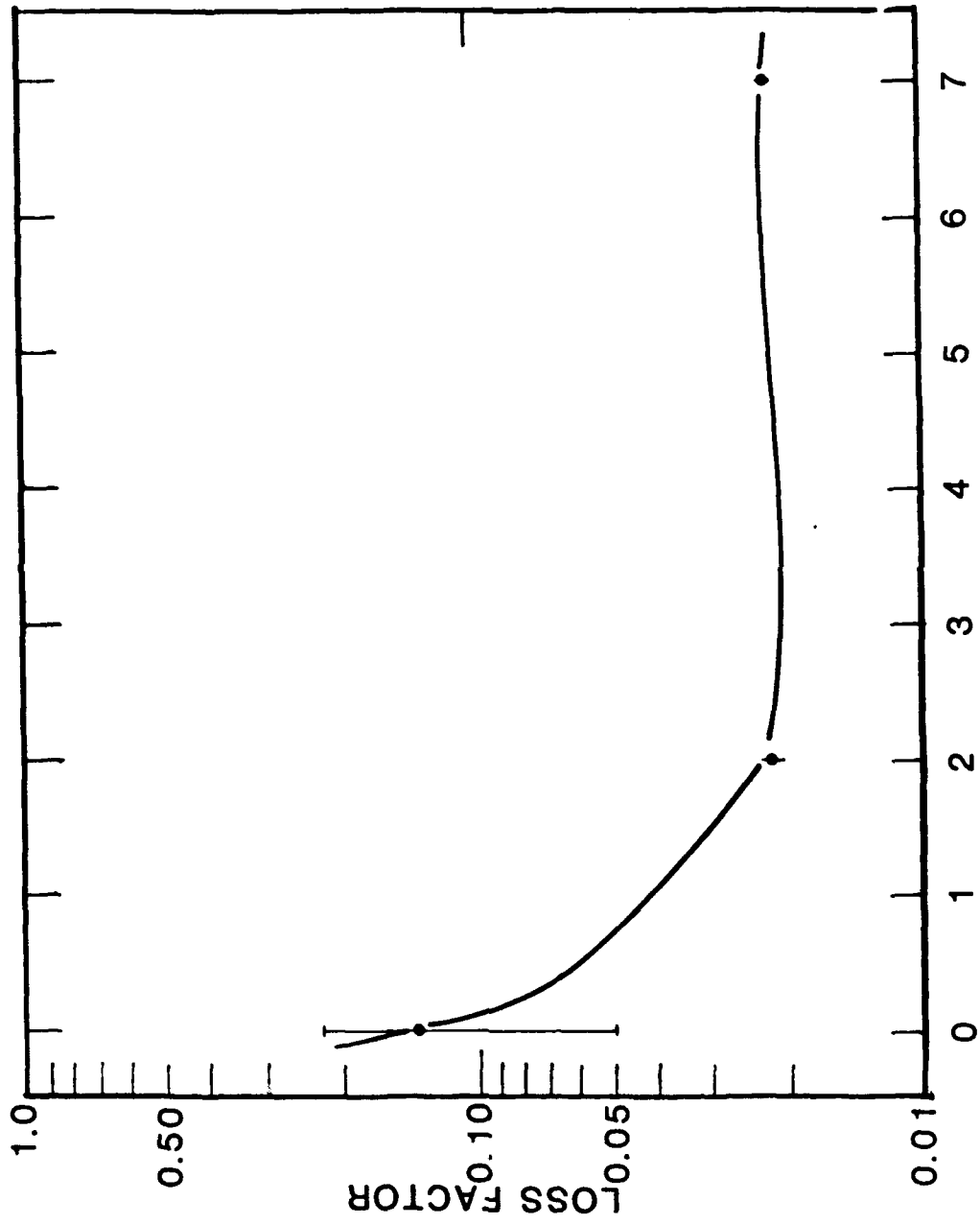

Figure 29. Effect of adhesive degassing time (minutes) on joint damping.

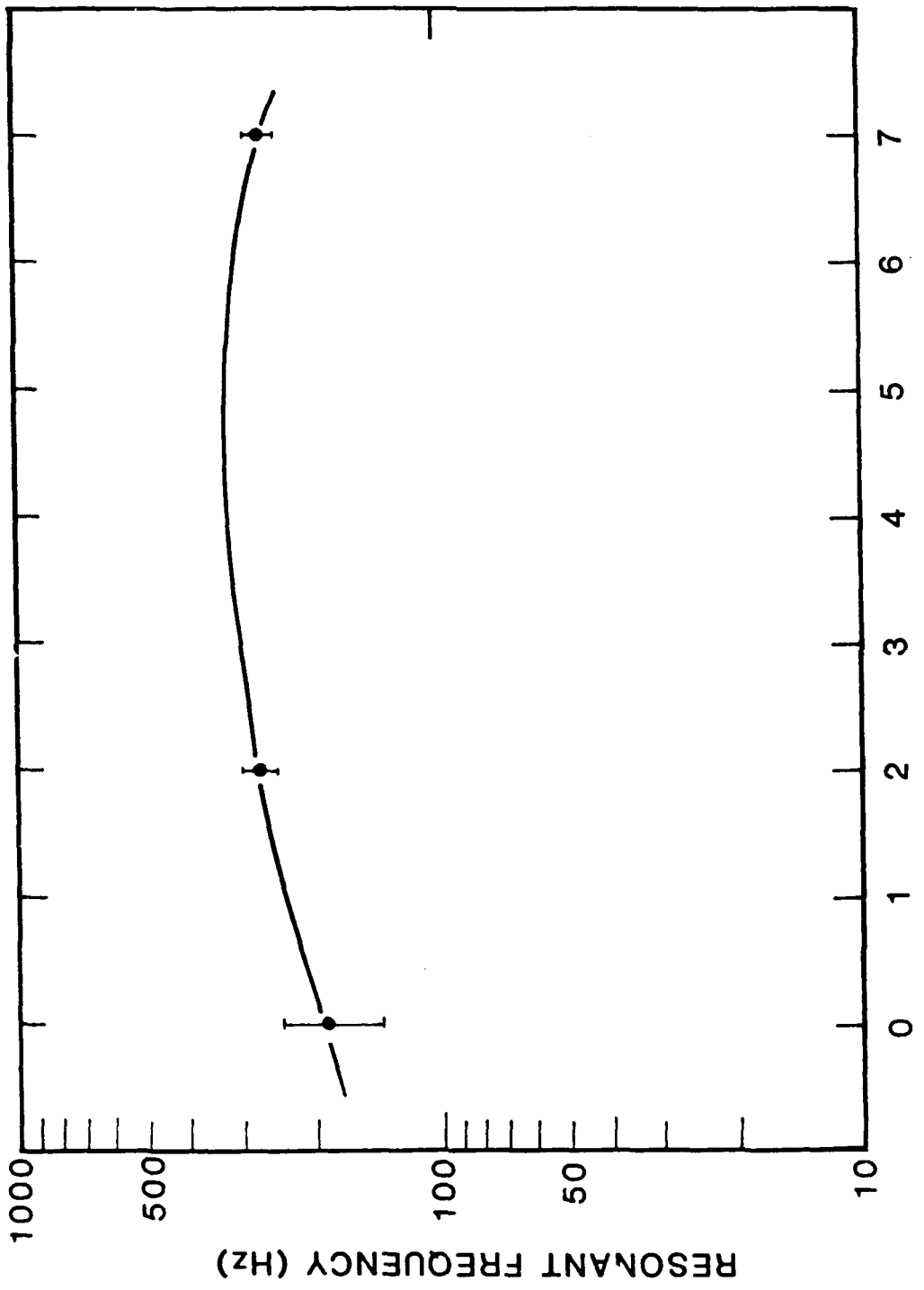

Figure 30. Variation of 1st mode resonant frequency (Hz) of adhesive joint with adhesive degassing time (minutes).

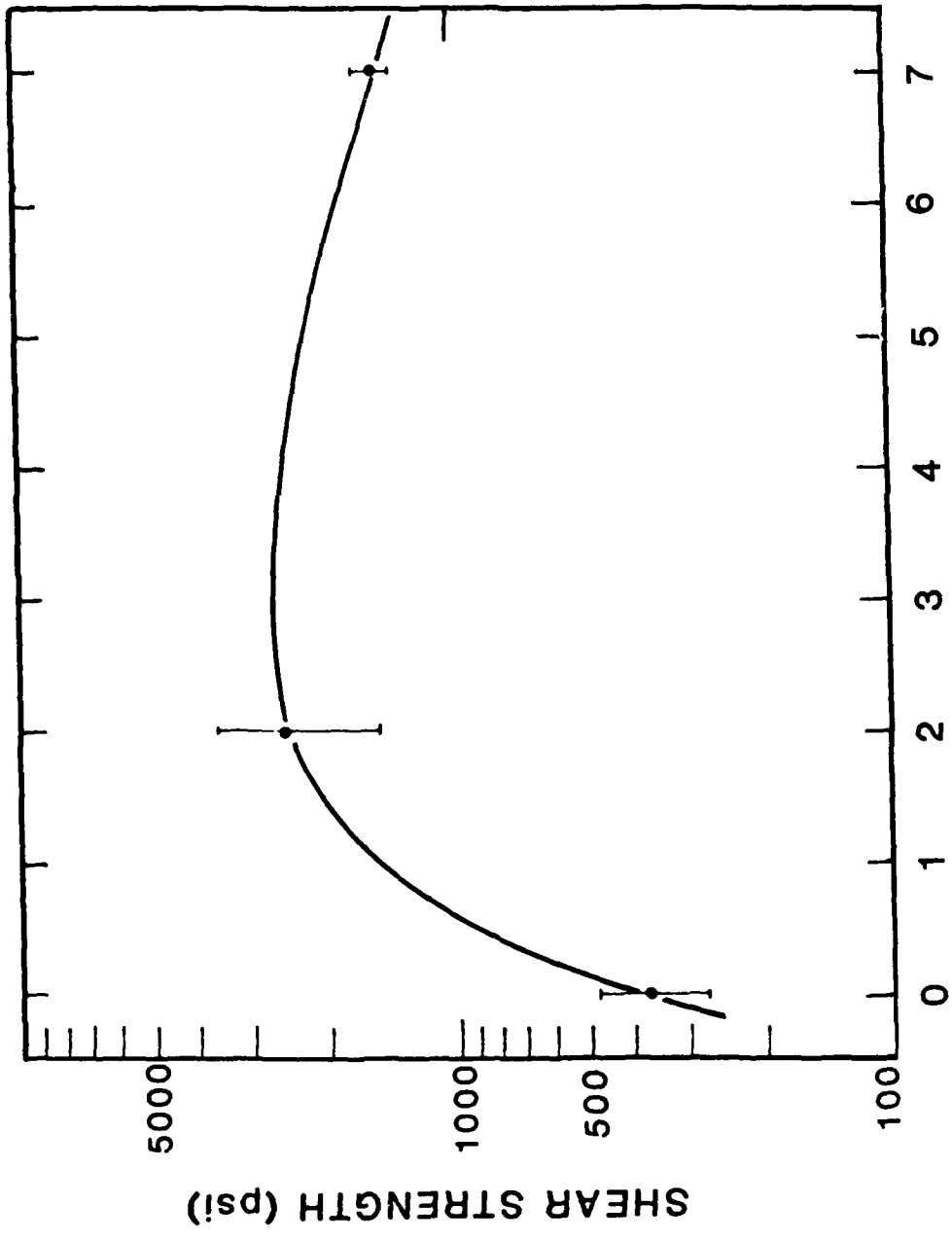

Figure 31. Variation of joint shear strength (psi) with adhesive degassing time (minutes).

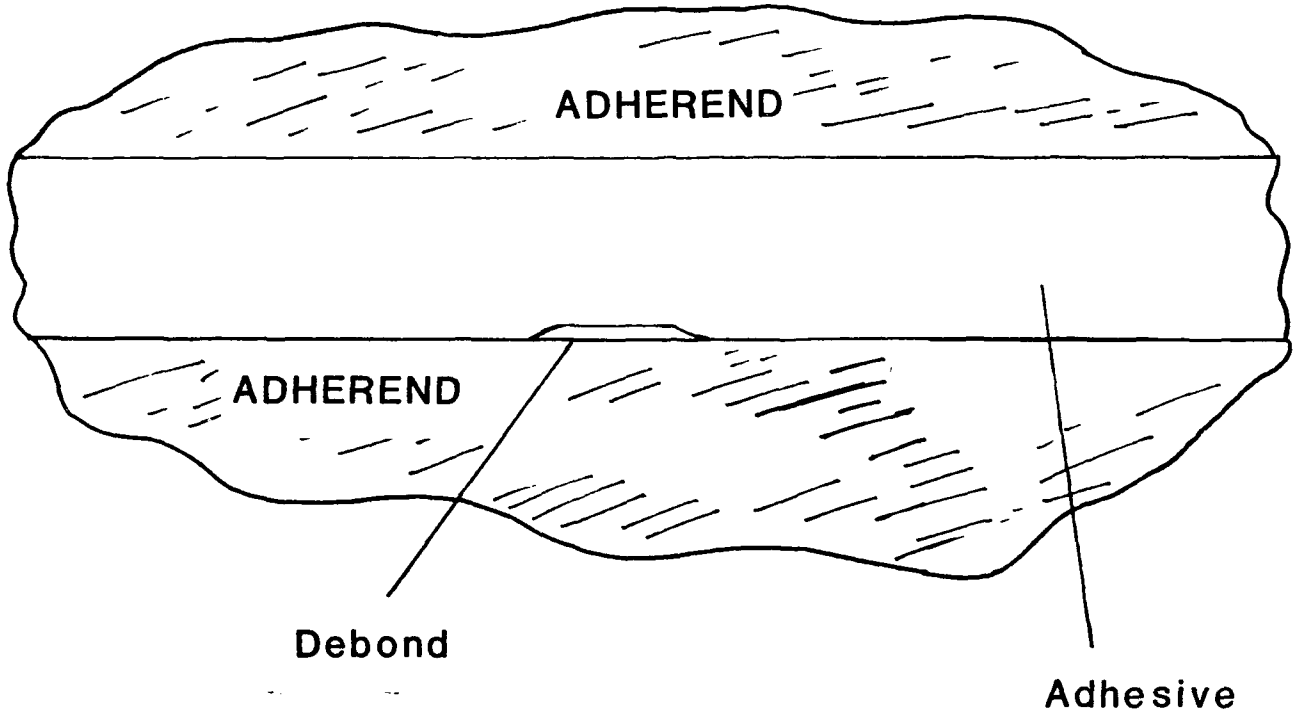

Figure 32. Typical defects: debond, caused by improper surface preparation.

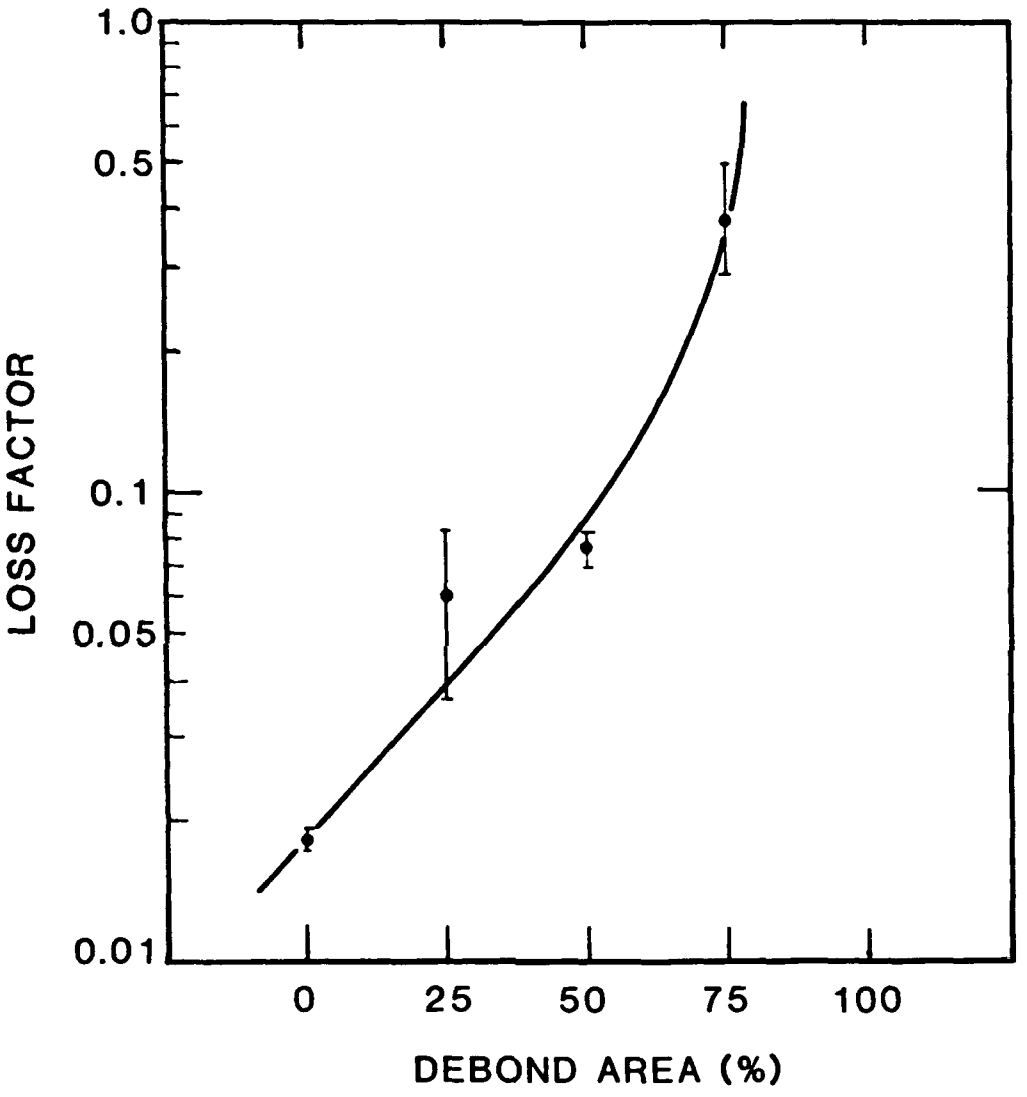

Figure 33. Effect of debond area (percent) on joint damping.

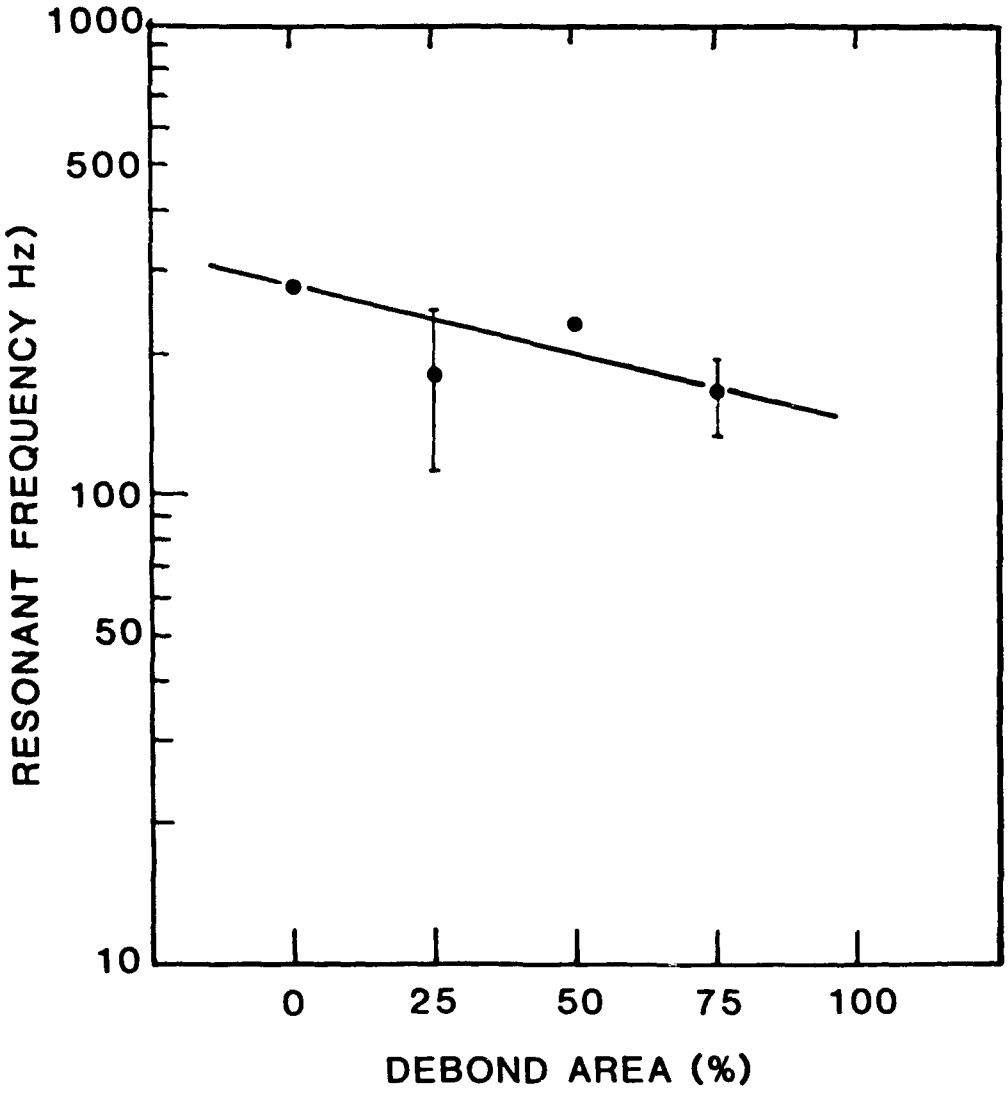

Figure 34. Variation of 1st Mode resonant frequency (Hz) of adhesive joint with debond area (percent).

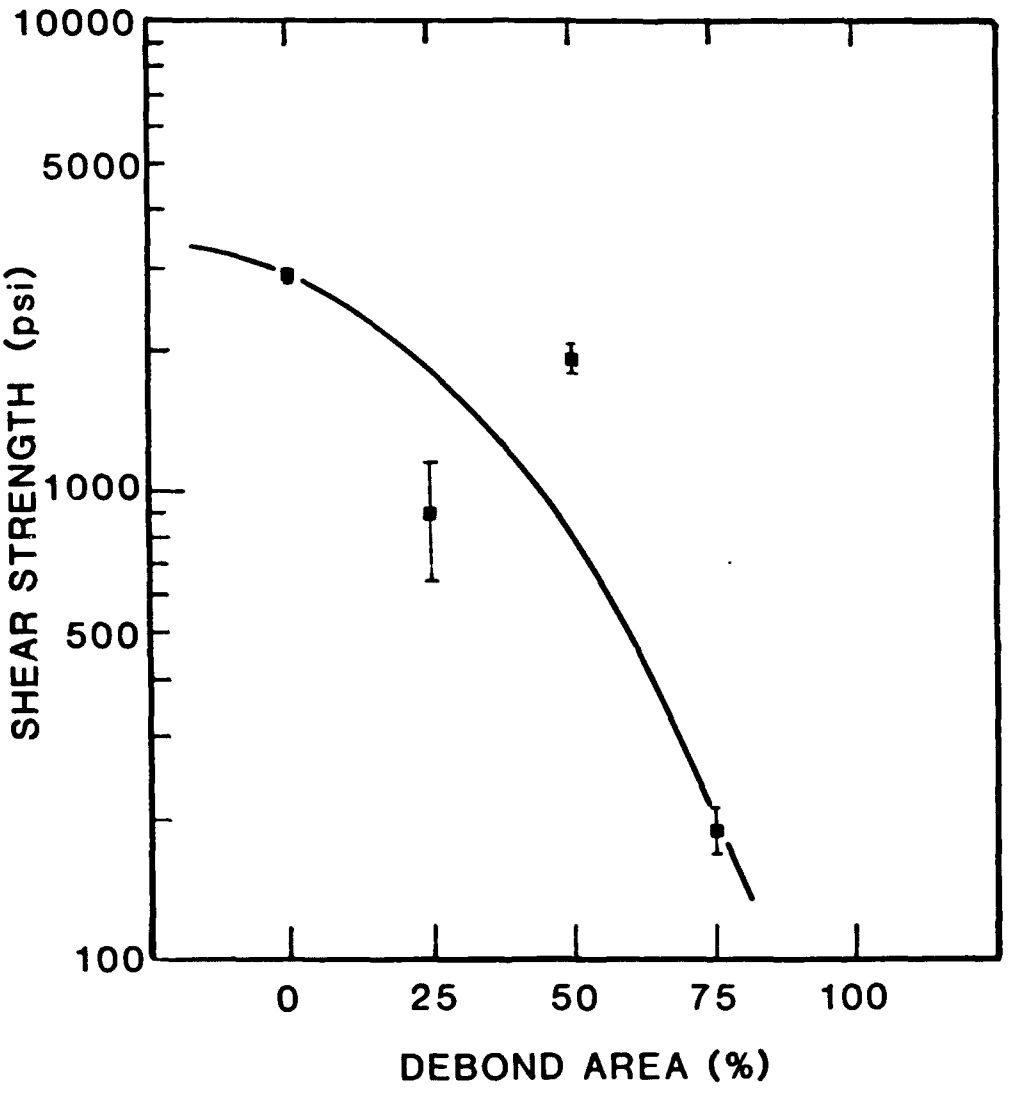

Figure 35. Effect of area of debond (percent) on joint shear strength (psi).

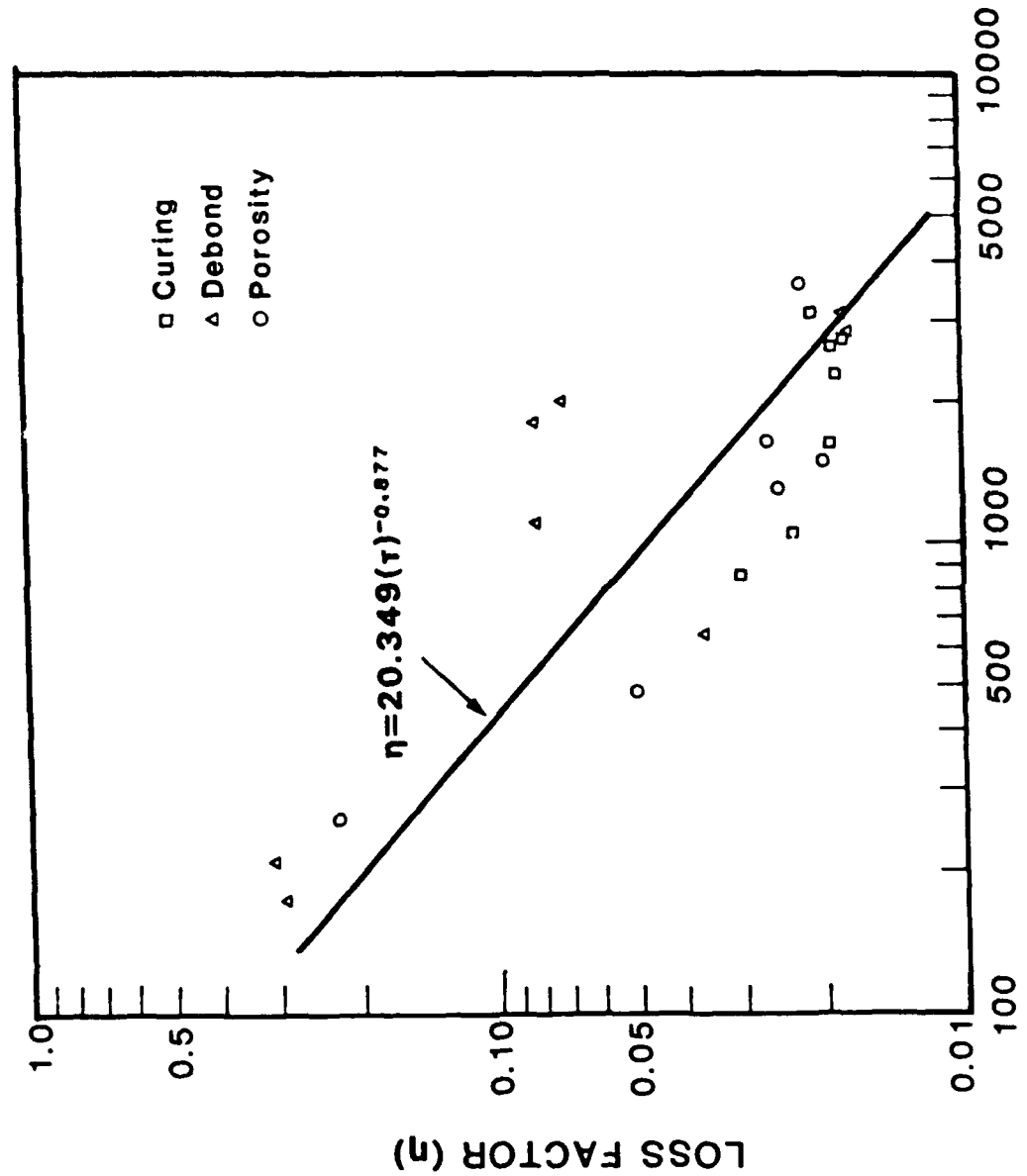

Figure 36. Variation of loss factor with joint shear strength for the double-lap joint composite specimens having flaws of varying size, number and degree of severity.

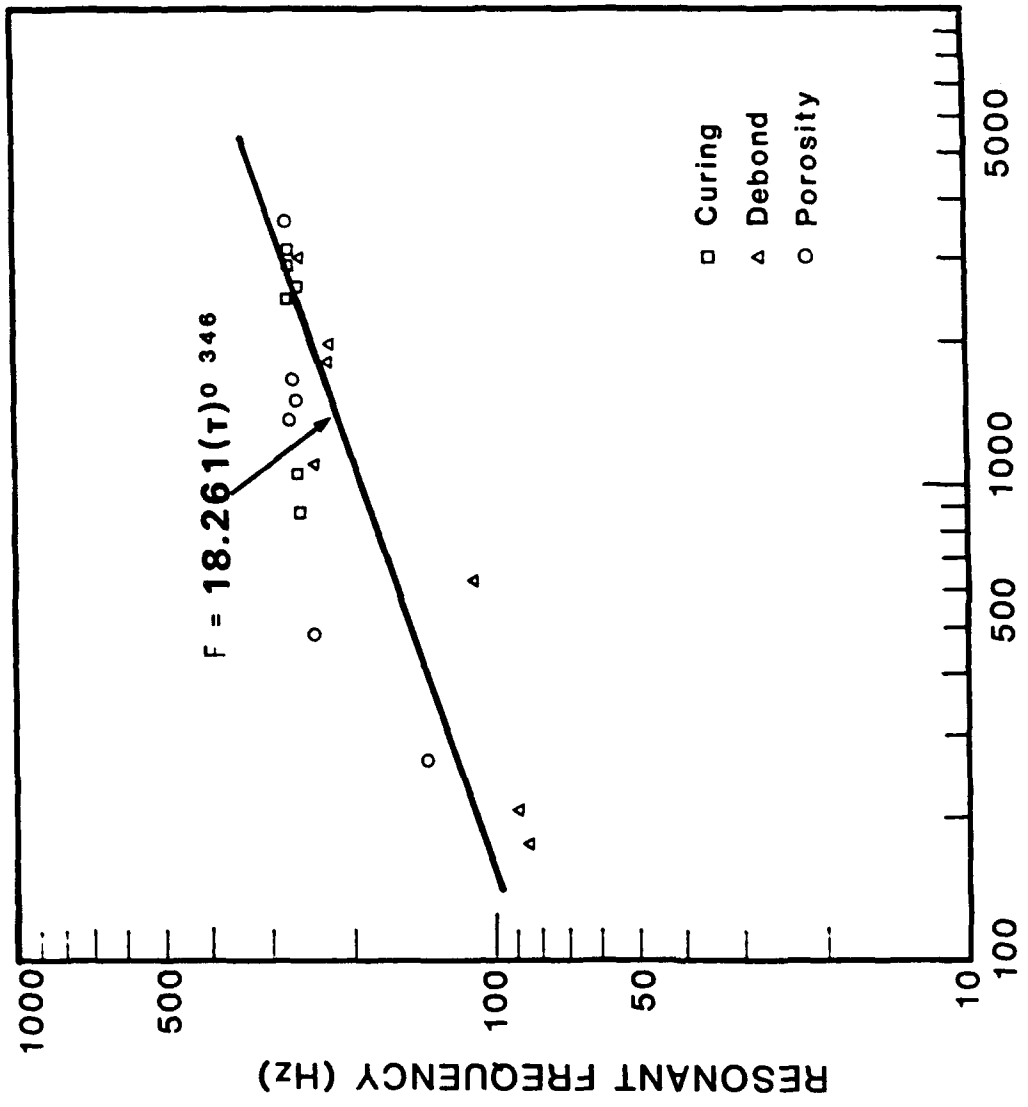

Figure 37. Variation of first mode resonant frequency with joint shear strength for the double-lap adhesive joint composite specimens having flaws of varying size, number and degree of severity.

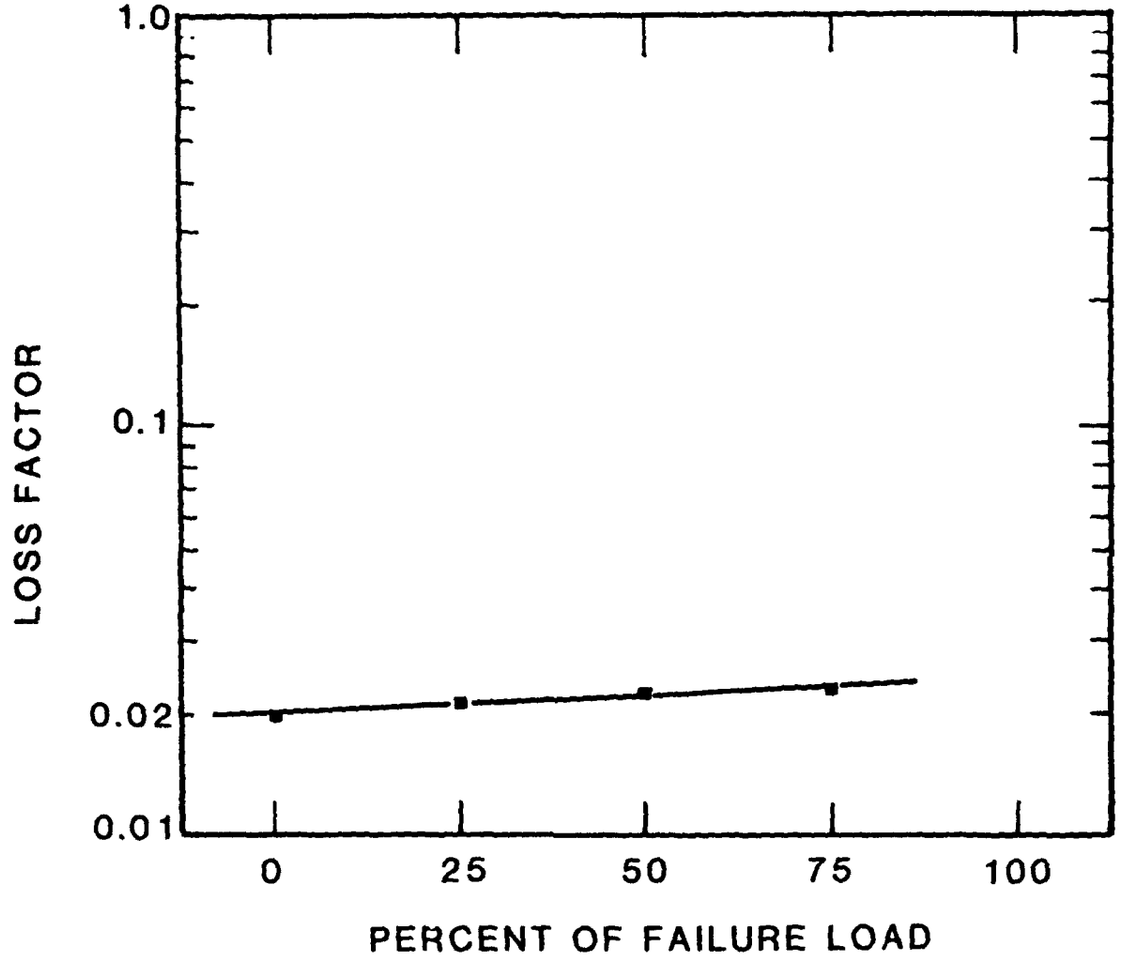

Figure 38. Effect of pre-load on joint damping.

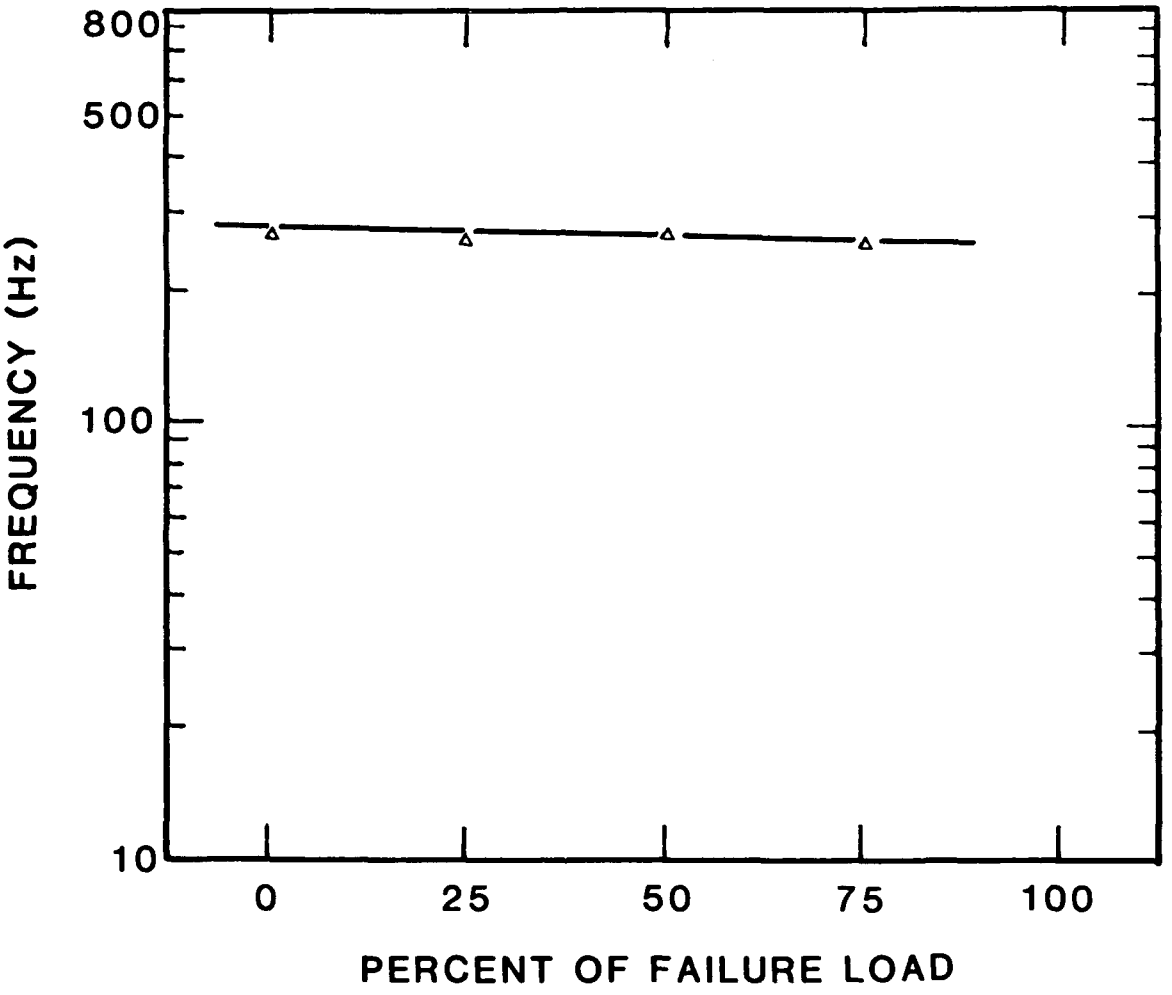

Figure 39. Effect of pre-load on joint 1st mode resonant frequency.

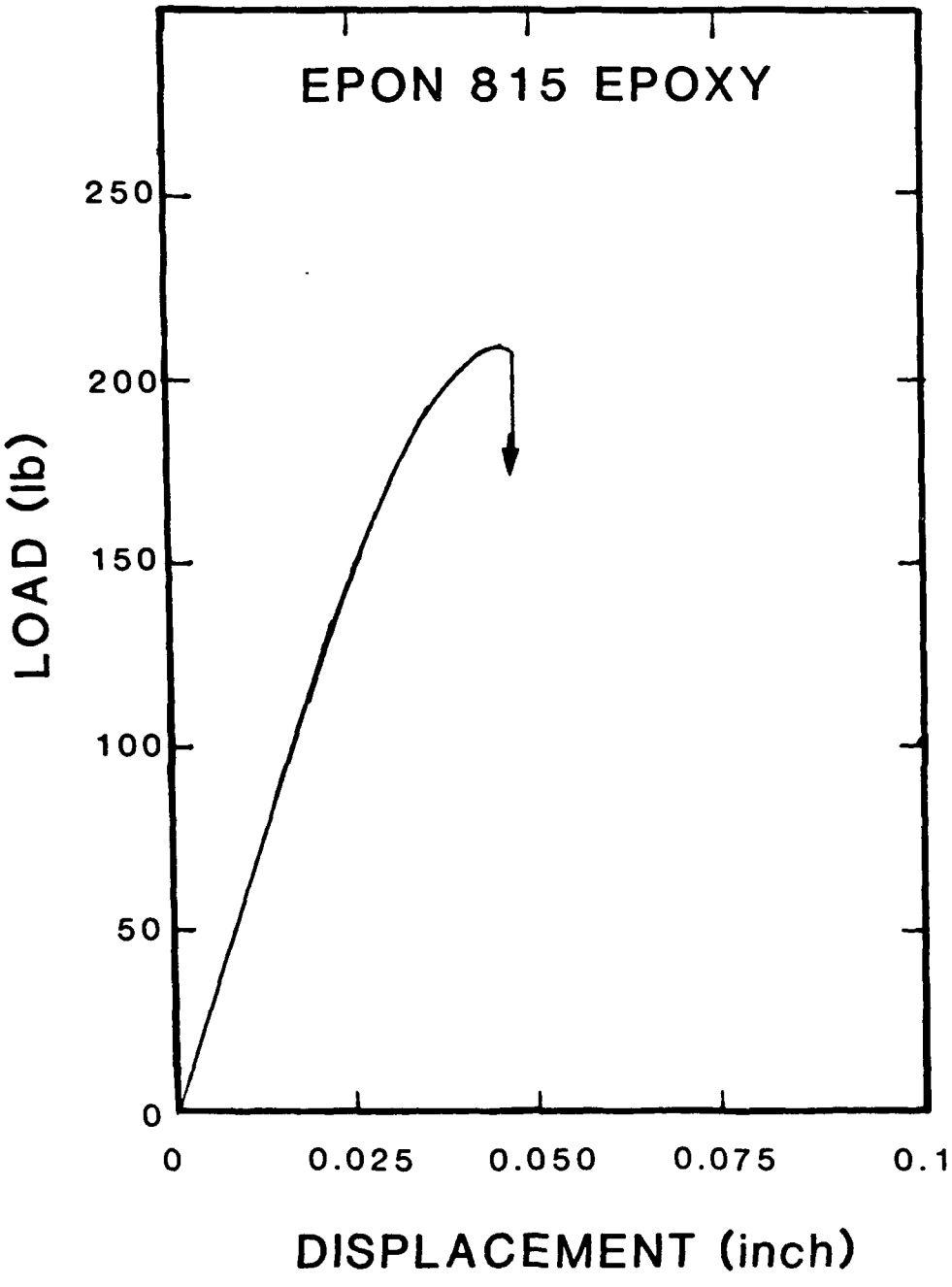

Figure 40. Load-Displacement curve for the EPON deformed in tension to failure.

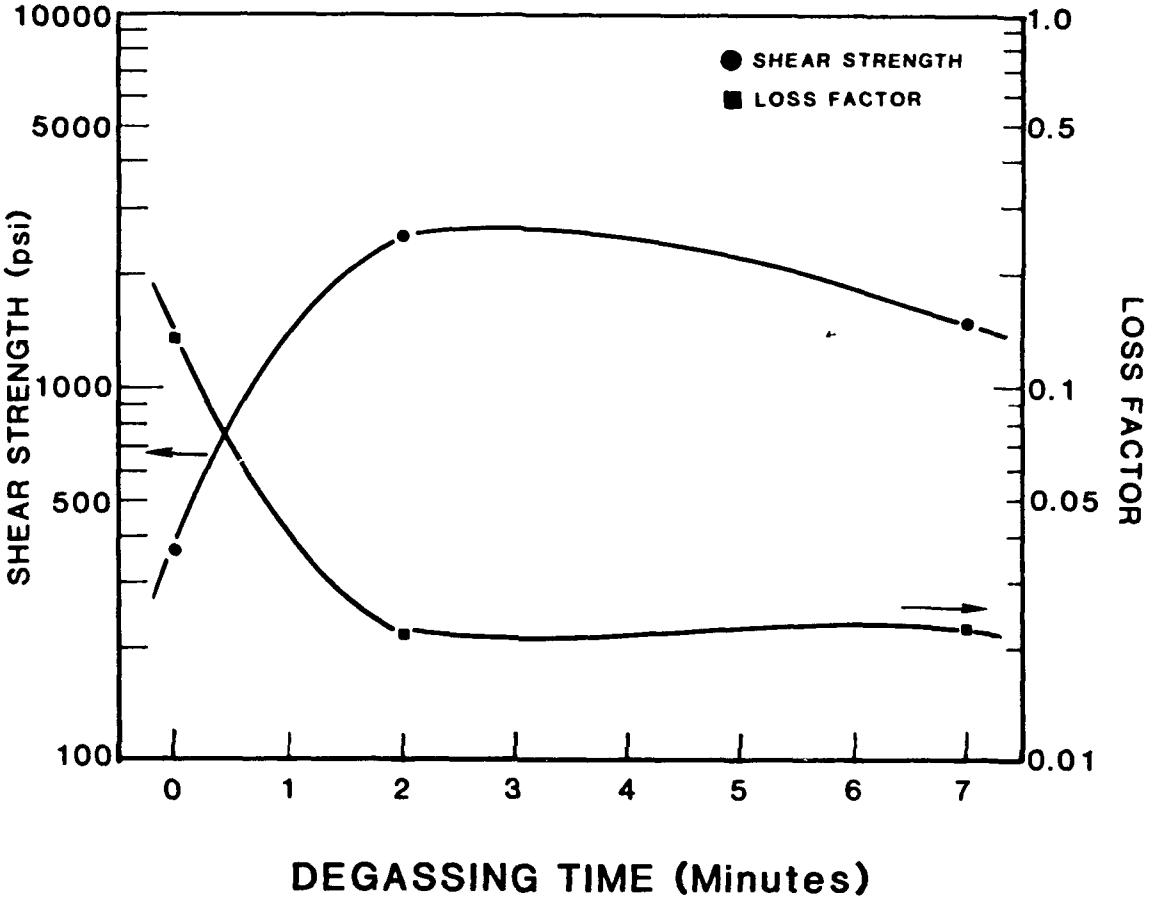

Figure 41. Comparison of the effect of adhesive degassing time on joint damping and joint shear strength.

Figure 42. Scanning electron micrograph showing fine microscopic pores in the specimen whose adhesive mixture was not degassed (Case: 0 minute degassing).

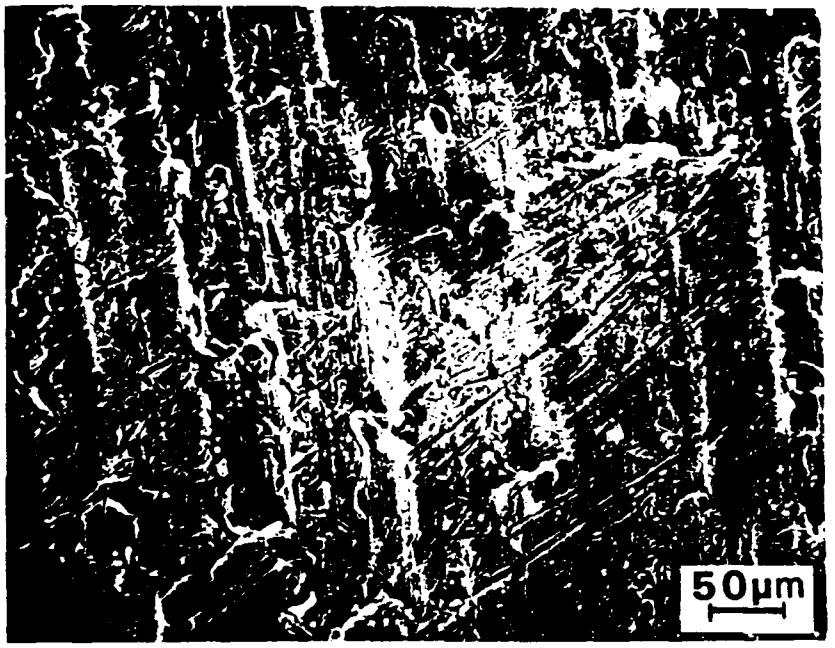

Figure 43. Scanning electron micrograph showing no evidence of pores in specimen whose adhesive mixture was degassed for 7 minutes.

The Composite Specimen

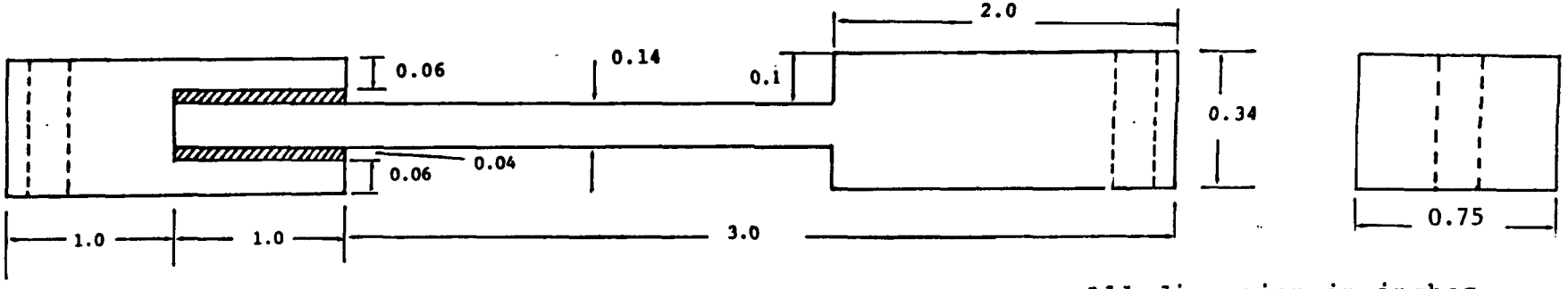

All dimension in inches.

Figure I - 1. Schematic showing dimensions of the adhesive layer and the adherend of the composite specimen. Figure is not to scale

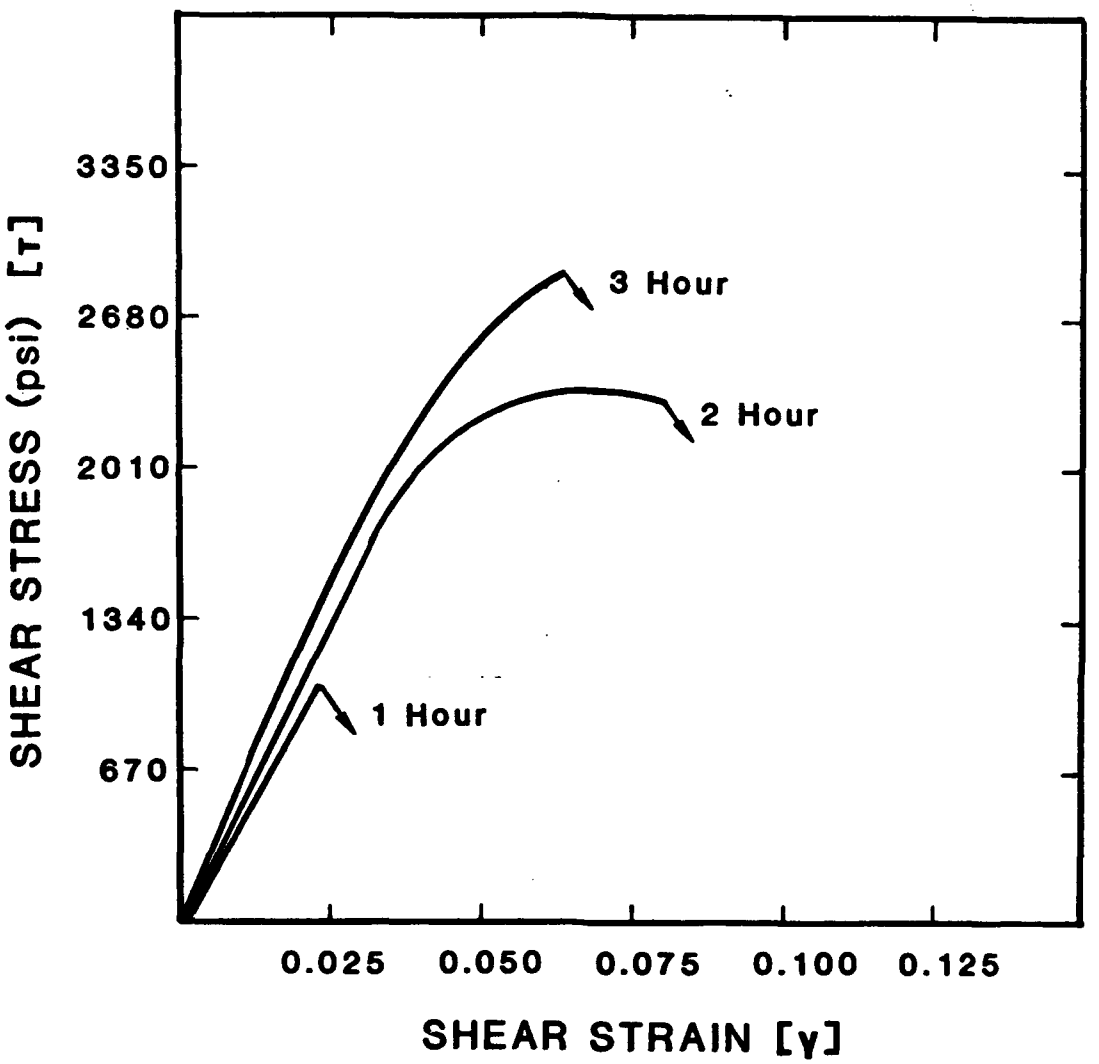

Figure II - 1. Comparison of representative shear stress-shear strain curves for the different cure times.

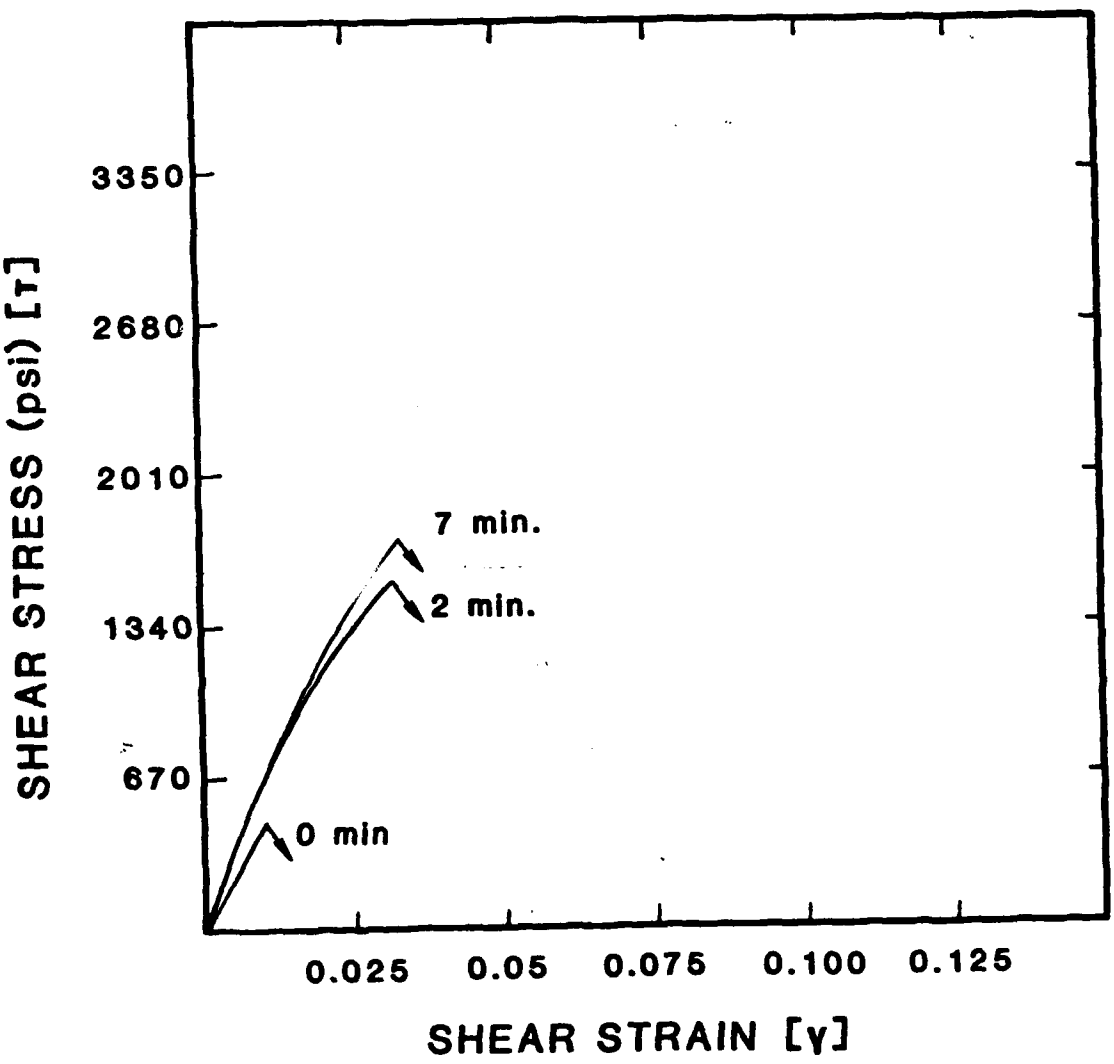

Figure II - 2. Comparison of representative shear stress-shear strain curves for the different degassing times.

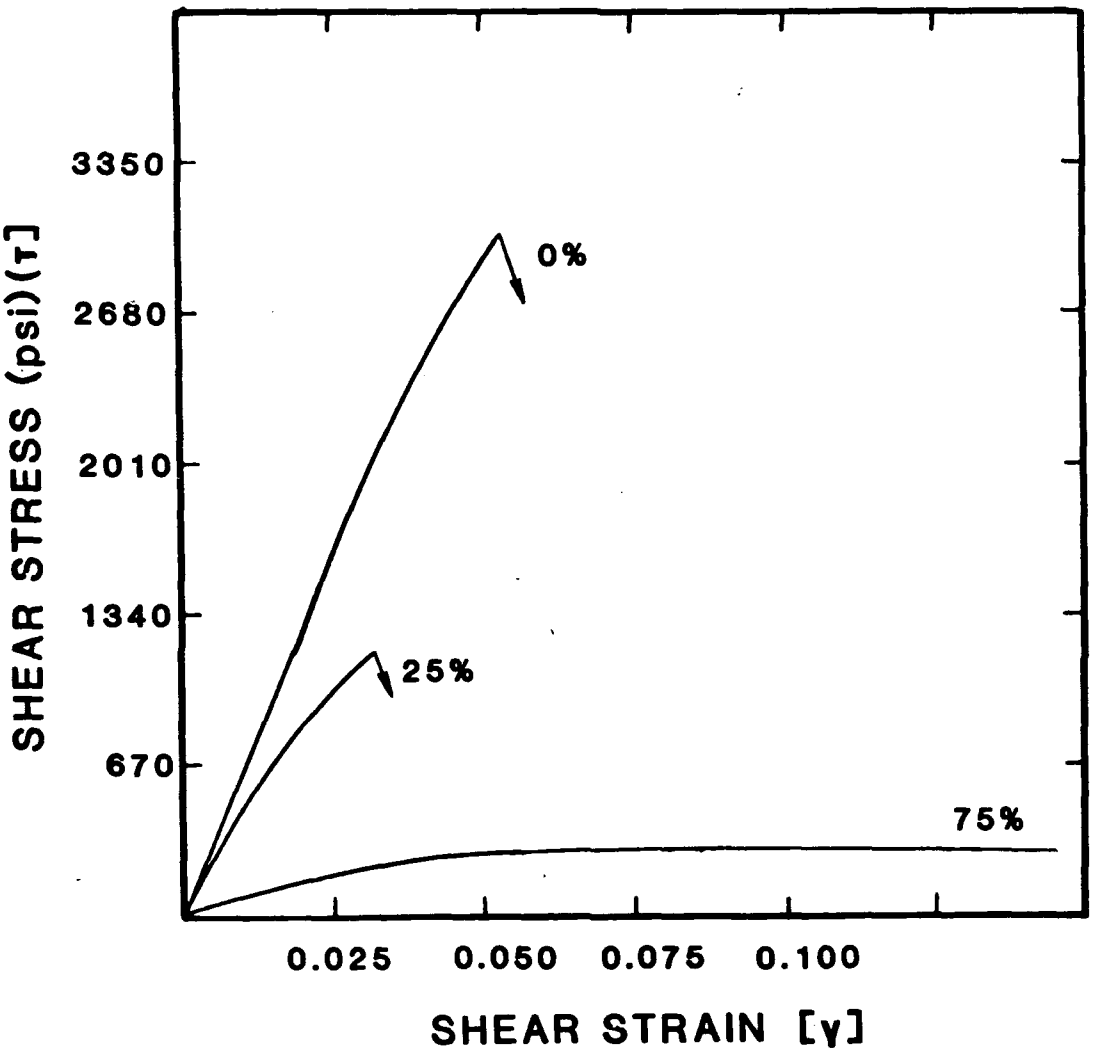

Figure II - 3. Comparison of representative shear stress-shear strain curves for the different amounts (%) of debond area.

Limitations of the Impulse Technique

The impulse-frequency response technique has proved to be quite valuable for both experimental vibration analysis and non-destructive testing of structures and machines. As with any experimental technique, however, the user must be aware of any limitations in order to obtain meaningful data. The most important limitations are summarized below.

1. The data reduction method assumes a linear system where both damping and stiffness are independent of vibration amplitude. Sources of damping other than material damping (e.g., friction in bolted joints, air damping, etc.) may not satisfy the linearity requirement. This limitation usually means that testing should be done at very small amplitudes. For example, air damping is negligible if the amplitude is less than about 10% of the component thickness.

2. Changes in damping only indicate the presence and severity of flaws or degradation. The location of such zones in the structure requires that more information be available. One possible source of this information is the mode shapes associated with each mode of vibration. The mode shapes govern the stress distribution, which in turn governs energy dissipation. For example, if a flaw is located at a point of zero stress for a particular mode of vibration, there will be no change in damping. On the other hand, if the flaw is located at a point of maximum stress for a particular mode, the change in damping will be maximized. Thus, by using the information on the damping, frequency and mode shape for each mode excited, the amount and location of damage can

be quantified.

3. If either the excitation or the response happens to be measured at a "nodal point" (a point of zero displacement) for a particular mode of vibration, the signal-to-noise ratio will be so low that the resulting data will be meaningless. Thus, a modal analysis of the structure is needed in order tc determine suitable measurement points for the NDE measurements.

4. In full scale component testing, the effects of boundary conditions is such that each type of component will probably have to be treated on an individual basis. For production line quality control testing, however, the boundary conditions can be specified and controlled so as to minimize this problem.

Recommendations for Future Work

Although the results of Phase I have demonstrated the feasibility of using damping measurements from the impulse technique for non-destructive characterization of flaws in adhesive joint specimens, there are several areas where future research is needed:

1. Characterization of Fatigue Damage

   Detection of the initiation and growth of cracks and debonds in adhesive joints under repeated loading is one of the key potential applications of the impulse technique. The demonstrated sensitivity of the method in detecting debonds in Phase I is an indication of its potential usefulness in the tracking of fatigue damage by periodic in-service inspection. The same double-lap joint specimens used in Phase I could be subjected to cyclic loading in our servo-hydraulic testing machine and periodic impulse test data could be correlated with damage growth.

2. Characterization of Environmental Effects

   The effects of environmental conditions such as temperature and humidity are important whenever adhesives are used. Our previous research on polymer matrix composites has shown that damping measurements are quite sensitive to such effects, and there is reason to believe that this conclusion would apply to joints as well. Our Phase I double-lap joint specimen could also be used here - the specimens would be subjected to varying temperatures and moisture concentrations

and impulse test data could be correlated with these control parameters. Temperature can be controlled by using electrical heaters and moisture content can be controlled by soaking the specimens in a water bath. Previous work on composites showed that the soaking method generated test data over the full range of moisture contents from fully dry to fully saturated.

In addition, environmental conditions could be used to accelerate fatigue damage growth.

3. Full Scale Component Testing

Since the major application of any NDE technique is to evaluate the structural integrity of components of structures and machines, the impulse technique must be tested on full scale components of interest to the funding agency. The effects of boundary conditions are expected to play a more important role in actual component testing than they have in tests of small specimens. For example, the damping due to friction at attachment points and the damping due to air drag are such that each type of component will have to be treated on an individual basis. For quality control inspections during fabrication of components, the boundary conditions can be specified so that this problem is minimized. Full scale component testing should also involve a complete "modal analysis". The presence of flaws or damage can be detected by damping measurements, but additional information is required for location of flaws or damage. The mode shapes associated with the different vibrational modes can be used as this additional information.

4. Interaction with Instrument Manufacturers Regarding Miniaturization for Portability

At some point, manufacturers of the equipment used in this research will have to be consulted regarding miniaturization of the computer - frequency spectrum analyzer system for enhancement of portability. The existing equipment is portable, but we feel that much could be done in the way of reducing the physical size of the package (e.g., could the whole thing be put on a chip?). Since the equipment we are using is manufactured by Hewlett Packard, that would be the logical place to start. Given the rapid changes in the electronics and computer industries, it may well be that such systems are already under development.